




RESEARCH ARTICLE OPEN ACCESS

Comparative Morphology of the Extrinsic and Intrinsic Leg Musculature in Dictyoptera (Insecta: Blattodea, Mantodea)

Fabian Bäumler¹  | Stanislav N. Gorb¹  | Sebastian Büsse^{1,2} 

¹Functional Morphology and Biomechanics, Institute of Zoology, Kiel University, Kiel, Schleswig-Holstein, Germany | ²Cytology and Evolutionary Biology, Institute of Zoology and Museum, University of Greifswald, Greifswald, Mecklenburg-Vorpommern, Germany

Correspondence: Fabian Bäumler (fbaeumler@zoologie.uni-kiel.de)

Received: 24 September 2024 | **Revised:** 17 November 2024 | **Accepted:** 21 November 2024

Funding: F.B. is directly supported by the Hans Böckler Foundation. The project is partially financed by the German Research Foundation (DFG) project BU3169/3-1 under project number: 531828325.

Keywords: *Chaeteessa* sp | cockroach | *Metallyticus splendidus* | praying mantis | predatory forelegs | prothoracic leg

ABSTRACT

Insect legs, as primarily locomotory devices, can show a tremendous variety of morphological modifications providing a multitude of usages. The prehensile raptorial forelegs of praying mantises (Mantodea) are a prominent example of true multifunctionality since they are used for walking while being efficient prey-capturing and grasping devices. Although being mostly generalist arthropod predators, various morphological adaptations due to different environmental conditions occur across Mantodea. Recently, the general mantodean morphology, and particularly their raptorial forelegs, received an increased interest. Yet, knowledge about the evolutionary transition from walking to prey-grasping legs is still scarce. From evolutionary and functional perspectives, the question arises: what changes were necessary to achieve the strongly modified raptorial forelegs—while keeping walking ability—and how does the foreleg morphology differ from the remaining four walking legs? In this context, we investigated the musculature of the raptorial forelegs in seven phylogenetically distant mantodeans, including pterothoracic legs in four of them, using high-resolution microcomputed tomography and dissection. To understand the results from an evolutionary perspective, we additionally examined all three pairs of unmodified walking legs of the closest sister group—Blattodea. We updated the knowledge of blattodean morphology, revealing differences in cuticle structures of the coxal articulation of the first pair of legs between the two orders and a shared musculature set-up in all pairs of legs among later-branching mantodeans. Interestingly, the early branching species *Metallyticus splendidus* and *Chaeteessa* sp. show several muscular characteristics, otherwise found exclusively in one or the other order, with a few procoxal muscles showing an intermediate state between the two orders. Studying the evolutionary transition from a walking leg to a raptorial leg will help to understand the character evolution of this highly specialized biomechanical system from a purely locomotory appendage to a multi-functional device with all related amenities and constraints.

1 | Introduction

Insect legs, primarily serving as locomotory organs, can exhibit a remarkable range of functional and morphological specializations (Chapman 1998; Cranston and Gullan 2014).

They are used for jumping in froghoppers (Cercopoidea) (Burrows, Shaw, and Sutton 2008; Gorb 2004), enable swimming in aquatic true bugs (Belostomatidae) (Cullen 1969), allow digging in mole crickets (Gryllotalpidae) (Zhang et al. 2019), or silk spinning in webspinners (Embioptera)

This is an open access article under the terms of the [Creative Commons Attribution-NonCommercial-NoDerivs](https://creativecommons.org/licenses/by-nc-nd/4.0/) License, which permits use and distribution in any medium, provided the original work is properly cited, the use is non-commercial and no modifications or adaptations are made.

© 2024 The Author(s). *Journal of Morphology* published by Wiley Periodicals LLC.

(Büsse et al. 2019), to name just a few examples. Despite these diverse leg adaptations to fit various tasks, walking continues to be an important function of almost all legs across insect species. A prime example of such multifunctionality is the development of raptorial forelegs, specialized for capturing prey, with praying mantises (Mantodea) being the best-known and studied insect group showing these modifications (Brannoch et al. 2017; Loxton and Nicholls 1979; Prete 1999; Wieland 2013). While being highly adapted to capturing prey (Prete 1999), the mantodean's forelegs kept their purpose as locomotory organs (Rossoni and Niven 2022). In this context, the functional transformation from the walking legs of a dictyopteran-like ancestor to a mantodean-like raptorial foreleg is particularly interesting (M. Hörnig et al. 2018; Hörnig, Haug, and Haug 2017; Izquierdo-López et al. 2024; Zhang, Schneider, and Hong 2013). Unfortunately, due to the small number of fossil records of mantodean species in combination with their insufficient quality (e.g., fossils missing important morphological traits like parts of the forelegs), knowledge about the origin and course of morphological changes of the raptorial appendages within this group is scarce and under discussion (Delclòs et al. 2016; Grimaldi 2003; M. K. Hörnig, Haug, and Haug 2017). Although not conclusively resolved, previous studies proposed an origin of raptorial forelegs in the mantodeans dictyopteran-like ancestors between the Late Jurassic and Early Cretaceous (Demers-Potvin et al. 2021; Grimaldi 2003; Izquierdo-López et al. 2024; Legendre et al. 2015). One of the earlier studies has revealed an approximately 115-million-year-old species (*Raptoblatta waddingtonae*), showing an overall roach-like appearance while featuring a raptorial and mantodean-like foreleg morphology, potentially representing a close mantodean relative (Dittmann et al. 2015; Hörnig, Haug, and Haug 2017; Izquierdo-López et al. 2024). Together with the discovery of *Divocina noci* LIANG, VRŠANSKÝ AND REN 2012 and *Santanmantis axelrodi* GRIMALDI, 2003 it could potentially support a step-wise evolution of the modification of walking legs to today's raptorial forelegs (Dittmann et al. 2015; Grimaldi 2003; Liang, Vrsansky, and Dong 2012). Recently, Izquierdo-López et al. (2024) identified the increased tibial curvature as one of the major morphological differences between mantodeans and non-mantodeans, based on a comprehensive morphometric analysis of fossil and recent Dictyoptera. In their work, they were further able to identify important morphological features of the largest family within the extant Mantodea—the Mantidea—stating that “... straight tibiae, long coxae, and long femora ...” could represent specific mantidean synapomorphic traits (Izquierdo-López et al. 2024).

In extant mantodeans, all three leg pairs exhibit the fundamental components typical of insect legs (Snodgrass 1935): coxa, trochanter, femur, tibia and tarsus terminating in the pretarsus with two claws (Figure 1a). All members of this group show shared morphological characteristics associated with the adaptation towards an ambushing hunting strategy (Hurd 1999). Mantises show a highly elongated prothorax that is flexibly connected to the pterothorax. This unique feature provides them with the necessary flexibility for precise aiming of the body axis towards and striking at their prey items (Roy 1999; Wieland 2013). The raptorial forelegs are

characterized by elongated coxa and femur, which significantly extend the range of attack (Brannoch et al. 2017; Roy 1999). Notably, both the femur and tibia are equipped with two rows of spines forming an effective catching basket (Brannoch et al. 2017). Furthermore, praying mantises exhibit a large number of extrinsic muscles, located in the prothorax, associated with the movement capability of the foreleg (mainly controlling movements of the coxa) (Bäumler, Gorb, and Büsse 2023; Frantsevich 1998). The importance of numerous extrinsic muscles for an increased range of movements becomes especially clear, when considering that the same number of muscles is controlling one leg segment (coxa), compared to the intrinsic musculature controlling four leg segments (trochanter, femur, tibia, tarsus)—as previously described, both intrinsic and extrinsic muscles consist of 15 muscles, respectively (Bäumler, Gorb, and Büsse 2023). As the initial link in the kinematic chain, coupled with the highly movable sclerites of the coxal articulation, the extrinsic muscles significantly contribute to the mantis' forelegs flexibility (Frantsevich 1998).

In contrast, the meso- and metathorax are rather short and morphologically alike (Wieland 2013). The walking legs (meso- and metathoracic legs) are less specialized compared to the forelegs, appearing fairly typical for insects (Brannoch et al. 2017), with the metathoracic legs usually being longer (Roy 1999). They consist of a slightly elongated and cone-shaped coxa, a small trochanter, femur and tibia that are most often elongated in different degrees and a tarsus that terminates in the pretarsus with two claws (Brannoch et al. 2017). Although praying mantises are primarily generalist arthropod predators, a strong adaptation especially regarding the shape and size of the raptorial forelegs occurs in some species (Brannoch et al. 2017; Oufiero 2020), resulting in distinct ecomorphs (Svenson and Whiting 2009; Wieland 2013). These different ecomorphs represent a specialization within praying mantises, connected to the environmental conditions or specific prey preferences—with typical specializations repeating themselves many times across the mantodean tree (Hurd 1999; Svenson and Whiting 2009; Wieland 2013). Additionally, the opposed rows of spines on the femur and tibia exhibit variations depending on the species, with highly enlarged and sclerotized spines (*Metallyticus splendidus*; Figure 1b), elongated and thin spines (*Chaeteessa* sp.; Figure 1h), or strongly reduced spines (*Amorphoscelis pulchella* GIGLIO-TOS, 1913; cf. Brannoch et al. [2017] Figure 7) (Roy 1999; Wieland 2013). Species can also exhibit differences in the proportion between leg segments (Oufiero 2020), with for example an extremely shortened tibia in *Hypsicorypha gracilis* (Oufiero 2020) (Figure 1e), as a possible adaption towards a preference for flying prey, or showing a differently shaped femur (e.g., the ventrally bulged femur of members of the genus *Metallyticus* [Figure 1b]). However, the origins of these ecomorphs are still unclarified and under discussion (Svenson and Whiting 2009).

Recently, our morphological understanding of the raptorial forelegs in mantodeans was advanced by focusing on so far understudied groups and using previously underutilized methods (Bäumler, Gorb, and Büsse 2023). This revealed new information covering the influence of the almost

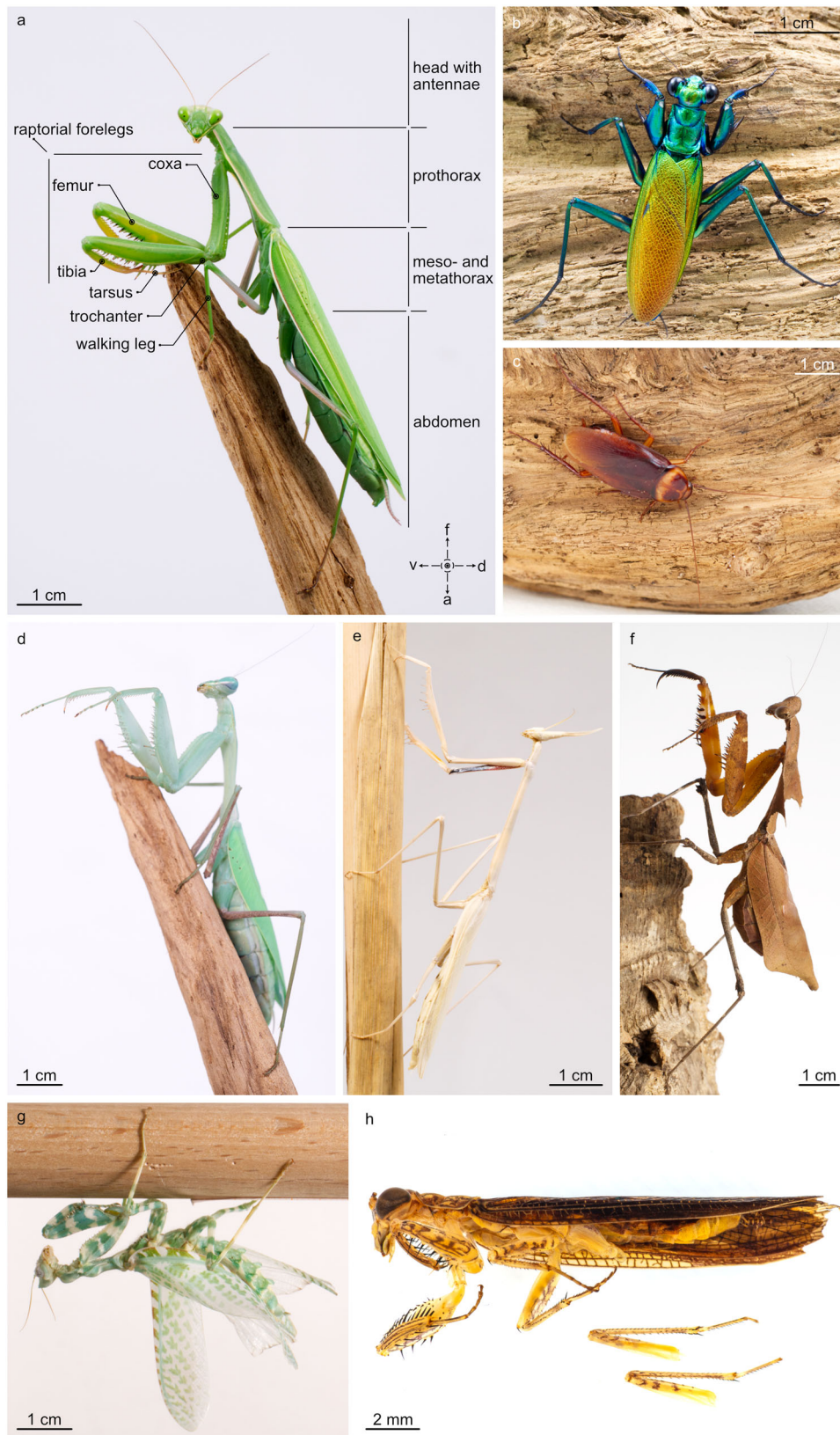


FIGURE 1 | Adult, female specimen of *Mantis religiosa* (a), *Metallyticus splendidus* (b), *Periplaneta americana* (c), *Hierodula membranacea* (d), *Hypsicorypha gracilis* (e), *Deroplatys desiccata* (f), *Blepharopsis mendica* (g) and *Chaeteessa* sp. (h) in lateral view. a, abdominal; d, dorsal; f, frontal; v, ventral.

ubiquitous sexual size dimorphism, as well as new insights into possible functionality of leg-controlling musculature. However, there is still a lack of information concerning the possible influence of the tremendous morphological variety

on ecological adaptations, especially concerning the raptorial forelegs. The initial transition of the latter has been poorly studied to date. Thus, the question arises: which morphological changes from the typical walking leg were

necessary to achieve a highly efficient prey-capturing device without losing the ability for locomotion? In contrast to the strongly modified raptorial forelegs of praying mantises, their phylogenetic sister group, the Blattodea, show unmodified walking legs. Due to their numerous preserved features, blattodeans were the subject of several entomological studies (Ariyanto et al. 2023; Carbonell 1947; Catania 2018; Delcomyn 1971; Full & Tu 1990; Jayaram and Full 2015; Jindrich and Full 1999; Weihmann et al. 2015). They are dorsoventrally flattened with some noticeable similarities of external features in comparison to mantodeans—for example, the highly mobile head articulation, the large compound eyes, as well as the enlarged pronotum with lateral suspensions (Carbonell 1947). Additionally, their thoracic musculature “... bears little resemblance to that of other insects.”, as Carbonell (1947) stated. Due to their phylogenetic relationship to the mantodeans, they represent the group of choice for a morphological comparison. Unfortunately, the majority of current publications document a high number of deviations in the reported musculature (Alsop 1978; Carbonell 1947; Frantsevich 1998; Maki 1938), which is why we included a blattodean taxon (*Periplaneta americana*) as an outgroup. In general, the transition from typical blattodean walking legs to raptorial forelegs in these closely associated groups of insects represents an interesting case of character evolution towards a functional specialization. Walking legs, which are primarily used for locomotion and support, have undergone a series of morphological and functional modifications, in terms of cuticular structures and presumably of muscular set-up, to become raptorial, specialized for capturing and manipulating prey (Rossoni and Niven 2022).

Here, we aim to bridge this knowledge gap, by first investigating the extrinsic and intrinsic musculature of the raptorial forelegs in different ecomorphs of several phylogenetically distant families within Mantodea. In our investigation, we covered species with raptorial forelegs in a “standard shape” (*Blepharopsis mendica*, *Deroplatys desiccata*, *Hierodula membranacea*, *Mantis religiosa*; Figure 1a,d,f,g)—a shape that can be found in a majority of mantodean groups—but also variations like *H. gracilis* (Figure 1e) with a comparably shortened tibia, *M. splendidus* (Figure 1b) with its enlarged spines and cockroach-like appearance, and *Chaeteessa* sp. (Figure 1h) with its long and thin spines, which is known to be the sister group of all remaining extant Mantodea (Brannoch et al. 2017; Svenson and Whiting 2009; Wieland 2013). As the main aim of this study is to understand the evolutionary transition from a walking leg to a prey-capturing device, we further included an analysis of the walking legs in mantodeans. Based on our observations, we present an updated overview of the extrinsic and intrinsic musculature in Blattodea, comparing the leg morphology and musculature of the two sister groups. We then discuss differences between blattodean to mantodean morphology and possible modifications that help understanding the multifunctionality in the raptorial forelegs of praying mantises. Our work will thereby ease future comparative and functional work, by providing a more solid base for approaches relying on knowledge of the musculature in Dictyoptera, and likely all Neoptera.

2 | Materials and Methods

2.1 | Specimens

Female specimens of the praying mantis species *Blepharopsis mendica* (FABRICIUS, 1775), *Deroplatys desiccata* WESTWOOD, 1838, *Hierodula membranacea* BURMEISTER, 1838, *Hypsicorypha gracilis* BURMEISTER, 1838, *Mantis religiosa* (LINNAEUS, 1758), and *Metallyticus splendidus* WESTWOOD, 1835, were obtained from private breeders or online shops and subsequently raised in Kiel to adulthood. A specimen of *Chaeteessa* sp. was provided by Dr. Jessica L. Ware from the collection of the American Museum of Natural History (NY, USA). All animals were kept in individual 19 x 19 x 19 cm “Braplast” (Terraristik Hörnchen GmbH, Bergheim, Germany) boxes, except for *M. splendidus*, which were kept in a group in a 40 x 40 x 40 cm glass terrarium. The containers were provided with 5 cm of coconut earth mixed with pine bark as floor ground and structured with sticks and plants and featured two mesh ventilation areas (one in the top back and one in the bottom front). The “Braplast” boxes further featured a 3D-printed feeding lid. The glass terrarium for *M. splendidus* was stocked with cork tubes and boards to create multiple crevices as hiding places. The containers were misted several times a week. Animals were kept at temperatures of ~21°C at night and up to ~27°C at day time, as well as a light:dark regime of 12:12 h. Tropical springtails (Collembola) and dwarf White isopods (*Trichorhina tomentosa* (BUDDÉ-LUND), 1893) were introduced to all containers for hygiene purposes as well as to serve as food for smallest larval stages. Mantises were fed two times a week with *Drosophila melanogaster* MEIGEN, 1830, in earlier larval stages, in later stages with *Drosophyla hydei* STURTEVANT, 1921, as well as blowflies (Calliphoridae) and *Thermobia domestica* (PACKARD, 1873). Additionally, female specimens of the blattodean species *Periplaneta americana* (LINNAEUS, 1758) were obtained from online shops for morphological investigations and were immediately fixed/frozen.

2.2 | Photography

Overview images of the animals (Figure 1) were done in a white light cube or an LED-dome system (Bäumler et al. 2020), using an Olympus OMD 10mkII digital camera (Olympus K.K., Tokyo, Japan), in combination with a Leica 45 mm macro lens (Leica Camera AG, Wetzlar, Germany) and Rotolights AEOS light sources (at 100%, 4500 K; Appleworld UK Ltd. Iwer Heath, UK). Subsequent postprocessing and labeling of the images were done using Affinity Designer 2 and Affinity Photo 2 (Serif [Europe] Ltd Nottingham, United Kingdom).

2.3 | Micro-Computed Tomography (μCT)

For μCT analysis, one adult female specimen of each species was initially euthanized using CO₂ before being fixed in Bouin's solution (=Duboscq-Brasil) (Romeis 1989). For post-fixation, specimens were washed and stored in a 70% ethanol solution. Before μCT scanning, an ascending ethanol series (70%, 80%, 90%, 95%, 99%, and 99%) was utilized to

dehydrate the samples, which were subsequently dried with a fully automatic Leica EM CPD300 critical point dryer (Leica, Wetzlar, Germany). To minimize vibrations, dried specimens were embedded in a semi-soft shoe cleaning foam (domol Schmutzradierer, Rossmann home brand domol, Dirk Rossmann GmbH, Burgwedel, Germany). Scanning was carried out using a Skyscan 1172 micro-CT (Bruker micro-CT, Kontich, Belgium; CT-scanner settings: X-ray source: 40 kV, 250 μ A, 360° rotation, 0.2 rotation step; image pixel size: *B. mendica*: 4.35 μ m; *D. desiccata*: 6.69 μ m; *Chaeteessa* sp.: 2.54; *H. membranacea*: 6.69 μ m; *H. gracilis*: 5.35 μ m; *M. religiosa*: 6.69 μ m; *M. splendidus*: 6.67 μ m; *P. americana*: 6.69 μ m). Cross-sectional images were initially reconstructed using Nrecon 1.0.7.4 (Bruker micro-CT, Kontich, Belgium), then processed in Amira 6.2 (Thermo Fisher Scientific, Waltham, Massachusetts, USA), using the brush and magic wand tool of the program's segmentation editor. After completing the analysis, individual surfaces of all the structures were created, using Amiras module "Generate Surface" (Unconstrained Smoothing, Smoothing Extent: 2), and subsequently exported as ".obj" files. The resulting files were imported into Blender 4.2 LTS (Blender Foundation, Amsterdam, Netherlands) for visualization. In Blender, all structures were given different colors, shadings and transparency for the cuticle was necessary, to ease a differentiation in the final figures. The labeling and arrangement of different images into a figure was done in Affinity Designer 2 (Serif [Europe] Ltd Nottingham, United Kingdom).

2.4 | Manual Dissection

To corroborate the findings, especially muscle attachment points, supplementary specimens were frozen at -70°C and after thawing subsequently dissected using a stereomicroscope and fine dissecting tools.

2.5 | Nomenclature

In descriptions of morphological characters, it is assumed that the orientation of the forelegs is consistent with a typical walking leg, as proposed by Wieland (2013). In this context, the stationary end of a muscle will be termed the point of origin (O), while its movable end will be termed the point of insertion. The conditions present in *Hierodula majuscula* (visualizations can be found in Bäumler, Gorb and Büsse [2023]) and *D. desiccata* are used as a reference in the descriptions of the musculature in the results section. Additional details and deviations attributed to species differences will be categorized under characteristics (C). The extrinsic muscles are named following the nomenclature established by Friedrich and Beutel (2008). The naming of the intrinsic muscles is based on the descriptions of Aibekova et al. (2022) and, following Friedrich and Beutel (2008), documented in supplementary online material Information 1. The terminology of cuticular structures employs the revised terminology introduced by Brannoch et al. (2017), supplemented by studies from Snodgrass (1935), Levereault (1936), Carbonell (1947), Gray and Mill (1985), Beutel et al.

TABLE 1 | Overview of used Abbreviations.

Term	Abbreviation
Accessory pleural apophysis lateral	apal
Accessory pleural apophysis ventral	apav
Basisternum	bs
Coxal foramen	cf
Coxo-trochanteral muscle	ctm
Dorso-ventral muscle	dvm
Epimeron	em
Episternum	es
Femoro-praetarsal muscle	fpm
Femoro-tibial muscle	ftm
Furca	f
Furca sternum	fs
Pleural apophysis	pa
Pleural ridge	pr
Pleurellite	pl
Pleuro-coxal muscle	pcm
Precoxal bridge	pb
Sterno-coxal muscle	scm
Supracoxal sulcus	scs
Tergal ridge	tr
Tergo-pleural muscle	tpm
Tergum	tg
Tibio-basitarsal muscle	tbm
Tibio-pretarsal muscle	tipm
Tibio-tarsal muscle	titm
Trochantero-femoral muscle	tfm
Trochantero-tibial muscle	ttn

(2014) and Wieland (2013). All relevant abbreviations are listed in Table 1.

3 | Results

The overall appearance of the animals is illustrated in Figure 1. For a comprehensive view of sclerites and cuticular structures, please refer to Figure 2 and the associated interactive 3D model, as well as Figure 3 in Bäumler, Gorb and Büsse (2023). For a supplementary comprehensive description of the sclerites, please refer to Carbonell (1947). Our investigation revealed a musculature configuration in mantodeans that is largely consistent with the most recent study of Bäumler, Gorb and Büsse (2023), showing notable similarities, but also distinct differences, particularly in comparison with cockroaches. Due to the low availability of specimens of *Chaeteessa* sp., we were only able to acquire one single specimen. Additionally, the specimen was not in an ideal condition (e.g., the hindlegs were already detached from the body). Unfortunately, in our analysis of the available data from this specimen, we could only determine the

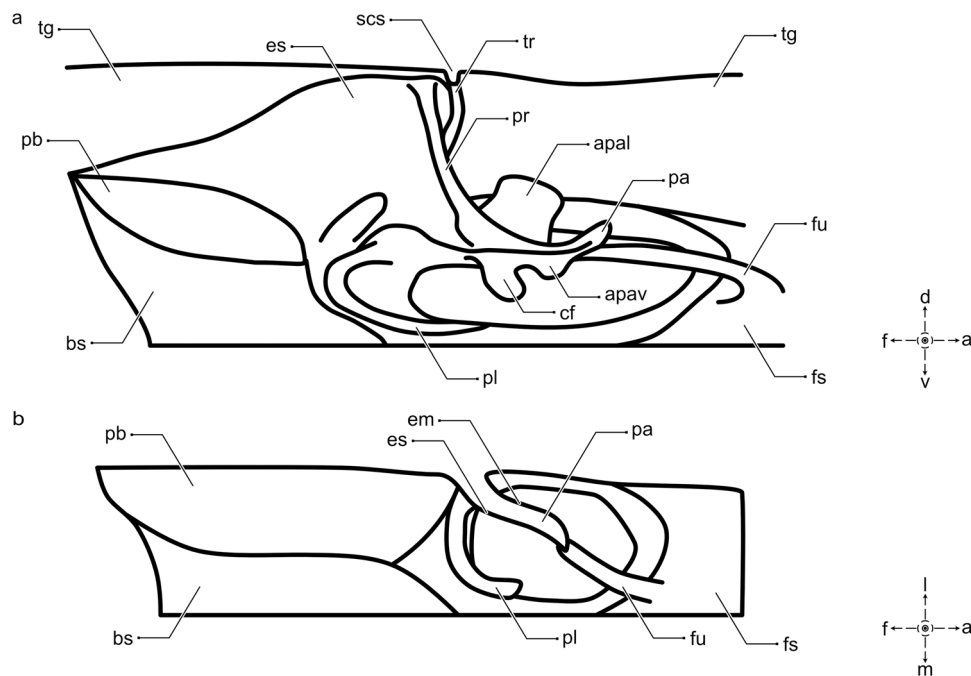


FIGURE 2 | Schematic drawing of the cuticle structures of the prothorax of Mantodea (a, medial view; b, dorsal view; modified after Carbonell [1947]). An additional interactive 3D model is available at (<https://skfb.ly/prRYQ>). a, abdominal; apal, accessory pleural apophysis lateral; apav, accessory pleural apophysis ventral; bs, basisternum; cf, coxal foramen; d, dorsal; es, episternum; em, epimeron; f, frontal; fu, furca; fs, furca sternum; l, lateral; m, medial; pa, pleural apophysis; pb, precoxal bridge; pl, pleurellite; pr, pleural ridge; scs, supracoxal sulcus; su, supracoxal sulcus; tg, tergum; tr, tergal ridge; v, ventral.

extrinsic and intrinsic musculature (excluding tibial muscles) of the prothorax for this species. Therefore, in the upcoming descriptions of the muscles in the meso- and metathorax, no information for *Chaeteessa* sp. is available. In total, we confirmed for all mantodeans 17 extrinsic (18 extrinsic for *Chaeteessa* sp.) and 13 intrinsic (15 intrinsic for *M. splendidus*; at least 11 for *Chaeteessa* sp.) muscles in the prothorax and the raptorial foreleg; 15 extrinsic and 15 intrinsic muscles in the mesothorax and mesothoracic leg (not determinable for *Chaeteessa* sp.) and 15 extrinsic and 15 intrinsic muscles in the metathorax and metathoracic leg (not determinable for *Chaeteessa* sp.). A 3D visualization for the musculature of *M. splendidus* can be seen in Figure 5, 6 and 7. In the representative of Blattodea (*P. americana*), we confirmed 17 extrinsic and 14 intrinsic muscles in the prothorax and prothoracic leg; 14 extrinsic and 14 intrinsic muscles in the mesothorax and mesothoracic leg and 13 extrinsic and 14 intrinsic muscles in the metathorax and metathoracic leg (Figure 3 and 4). Notably, while the number of muscles may coincide in some cases, the specific muscle presence/absence can vary, even within Mantodea, as seen in *Chaeteessa* sp. and *M. splendidus*. The differing coxal musculature of *Chaeteessa* sp. and *D. desiccata*, (as an example for the remaining later branching mantodeans), that will be elaborated in the discussion part, can be seen in the following interactive 3D models: <https://skfb.ly/p8FCA> and <https://skfb.ly/p8FC7>. A detailed description of the musculature of individual species is presented below and in Supporting Information Online Material, Supporting Information S1: 1.

Despite the apparent uniformity of internal cuticle structures for muscle attachment in Mantodea, the Blattodea as their sister group, show some distinct differences. The thorax of *P.*

americana shows several preserved features and is relatively typical for a generalist insect, lacking the elongated prothorax found in mantodeans. In *P. americana*, the internal sclerites, particularly the furcae, are notably elongated and narrowing towards the tip in all thoracic segments, extending towards the pleural apophysis, which arises from the pleural ridge dividing the prothoracic pleuron into the anterior episternum and the posterior epimeron (Supporting Information S1: 2).

Due to the greatly elongated prothorax, some internal sclerites are shifted in Mantodea. The prothorax is mechanically stabilized by a huge internal sclerite—the transversal ridge (cf. Frantsevich [1998]), an apomorphic feature of mantodeans—extending from the dorsal junction of the tergal and pleural ridge down to the lateral coxal articulation point, stretching anterior up to the cervical rim. The ridge is externally visible from the dorsal view, forming the supracoxal sulcus that divides the pronotum into pro- and metazone. It represents a fused structure made from tergal, pleural and sternal sclerites. In the dorsal area, the transversal ridge is laterally reinforced by a V-shaped longitudinal infolding, partially compromised of the tergal and the pleural ridge (Figure 2) (Leverault 1936); named “pleural crista” in Friedrich and Beutel (2008). The strongly enlarged and thickened pleural ridge protrudes deep into the prothoracic cavity, with its associated pleural apophysis elongated posteriorly and positioned more ventrally compared to *P. americana*. In the most ventral area, the pleural ridge forms the main lateral articulation point of the procoxa (coxal foramen, Figure 2 and Supporting Information S3: 3). Posteriorly of this articulatory point, the ventral part of the episternum (part of the pleurellum) is in close contact with

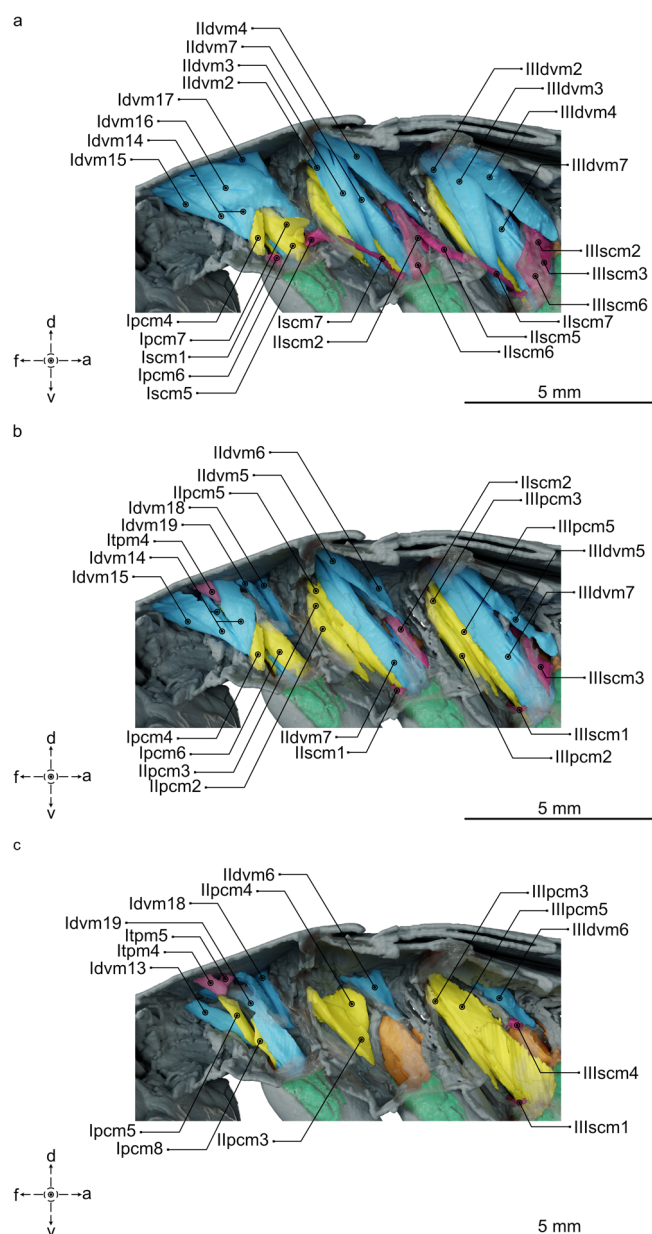


FIGURE 3 | Three-dimensional visualization of the extrinsic musculature in the thorax of an adult female *Periplaneta americana* from μ CT data in medial view. Partially, the cuticle is displayed transparent, to allow for a better view of the musculature in the back layers. Muscles are subsequently removed in every layer, to enhance an understanding of the spatial arrangement. (a) first layer; (b) second layer; (c) third layer. Additional interactive 3D models are available here: Extrinsic musculature of the prothorax (1 [<https://skfb.ly/prQMw>] and 2 [<https://skfb.ly/prQMz>]), the mesothorax (1 [<https://skfb.ly/prRRr>] and 2 [<https://skfb.ly/prQMF>]) and the metathorax (1 [<https://skfb.ly/prRRB>] and 2 [<https://skfb.ly/prQNN>]). a, abdominal; d, dorsal; dvm, dorso-ventral muscle; f, frontal; pcm, pleuro-coxal muscle; scm, sterno-coxal muscle; tpm, tergo-pleural muscle; v, ventral.

the pleural apophysis, forming a ventral as well as a lateral protrusion for muscle attachments. Here, the pleural process and the tip of the elongated furca are also in close contact and not easily separated in the dissection. Interestingly, the described articulatory point is slightly rotatable in

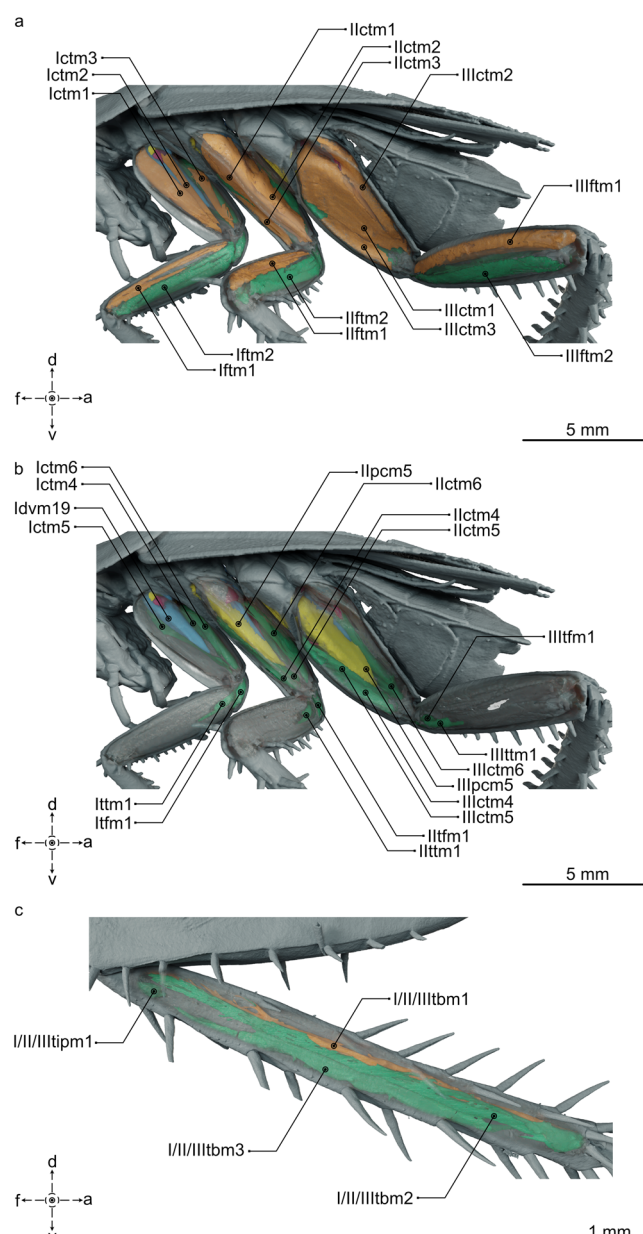


FIGURE 4 | Three-dimensional visualization of the extrinsic musculature in the thorax and the intrinsic musculature in the legs of an adult female *Periplaneta americana* from μ CT data in medial view (a and b show coxa, trochanter and femur; c shows the tibia). Partially, the cuticle is displayed transparent, to allow for a better view of the musculature in the back layers. Muscles are subsequently removed in every layer, to enhance an understanding of the spatial arrangement. (a) first layer; (b) second layer; (c) tibia. Additional interactive 3D models are available here: Intrinsic musculature of the foreleg (<https://skfb.ly/prQM7>), midleg (<https://skfb.ly/prQMr>), hindleg (<https://skfb.ly/prQMq>) and exemplary tibial musculature of the hindlegs (<https://skfb.ly/prRRP>). a, abdominal; ctm, coxo-trochanteral muscle; d, dorsal; dvm, dorso-ventral muscle; f, frontal; ftm, femoro-tibial muscle; pcm, pleuro-coxal muscle; tbm, tibio-basitarsal muscle; tpm, tergo-pleural muscle; tfm, trochantero-femoral muscle; tipm, tibio-praetarsal muscle; ttm, trochantero-tibial muscle; v, ventral.

a longitudinal direction (Supporting Information S4: 4). The trochantine sclerite (pleurellite in Levereault [Levereault 1936]) is flexibly connected to the katepisternum and folds in ventro-laterally to form a knob-like

protrusion—the second and median coxal articulatory point (accessory pleural apophysis ventral, Figure 2 and Supporting Information S3: 3).

Both mantodeans and blattodeans use the pterothoracic (meso- and metathorax) legs for walking, and the musculature in those segments shows fewer differences between the two orders. The internal cuticular structures appear comparably similar: in both segments, the furcae are elongated and in close, but flexible contact with the pleural apophysis. In blattodeans, the pleural apophysis is short and situated in the dorsal area of the pleural ridge, and the furcae are further elongated in the dorsal direction. In Mantodea, the pleural apophysis is enlarged and situated in the ventral area of the pleural ridge. Furthermore, the walking legs (all legs of Blattodea but only pterothoracic legs of Mantodea) of both species show many similarities, especially the rather uncommon elongated and enlarged coxa and comparably big trochanter.

3.1 | Prothorax

Extrinsic musculature of the forelegs (Figure 3 and 5).

Dorso-ventral musculature

Idvm13—M. pronoto-trochantinalis anterior

O: Prothoracic episternum, postero-lateral of Idvm15.

I: On an apodeme of the anterior procoxal rim, close to Idvm15.

C: Muscle is much shorter and the attachment area is more lateral and closer to Idvm15 in *P. americana*, *Chaeteessa* sp. and *M. splendidus*.

Idvm14—M. pronoto-trochantinalis

O: With three prominent strands: at the median region of the prozone of the pronotum, anterior of the transversal ridge (at height of the pleural ridge), at the median part of tergum, close to and posteriorly of the transversal ridge and the median area of the metazone of the pronotum.

I: Trochantin, posterior of Idvm13.

Idvm15—M. pronoto-trochantinocoxalis

O: With two strands, at the lateral part of the prozone of the pronotum, antero-medial to Idvm13.

I: On an apodeme of the anterior procoxal rim, close to Idvm13.

C: The muscle is much shorter and the attachment area is more medial and closer to Idvm13 in *P. americana*, *Chaeteessa* sp. and *M. splendidus*.

Idvm16—M. pronoto-coxalis anterior

O: Postero-lateral part of the metazone of the pronotum.

I: At a tendon, connected to the postero-lateral procoxal rim.

C: Most posterior foreleg muscle, inserts posterior of Idvm17. In *P. americana*, it does not end in a tendon. In Mantodea, it shares the point of attachment with muscle Iscm2.

Idvm17—M. pronoto-coxalis posterior

O: Lateral part in the middle region of the metazone of the pronotum.

I: In a tendon, connected to the postero-lateral procoxal rim, anterior of Idvm16.

C: In *P. americana*, it does not insert in a tendon.

Idvm18—M. pronoto-coxalis lateralis

O: Postero-median region of the metazone of the pronotum.

I: Antero-lateral procoxal rim, antero-median of Ipcm.

C: Point of origin is considerably more lateral in *P. americana*.

Idvm19—M. pronoto-trochanteralis

O: With three strands: (i) lateral of the anterior area of the metazone of the pronotum, (ii) at the median part of the metazone of the pronotum, and (iii) at the metazone of the pronotum, lateral and very close to the Idvm14.

I: Together with Ipcm8, Iscm6, and Ictm5 at the trochanteral extensor apodeme.

C: The trochanteral extensor apodeme is much smaller and shorter in *P. americana*. Furthermore, the muscle is only two-stranded in *P. americana* (the median one is missing) and the strands are closer together.

Idvm20—M. pronoto-coxalis medialis

O: Postero-median region of the metazone of the pronotum, anterior to Idvm18 and posterior to Idvm16.

I: Antero-lateral procoxal rim and same attachment point as Iscm4.

C: The muscle is not present in *P. americana* but in all mantodeans; it was newly described for Mantodea (Bäumler, Gorb, and Büsse 2023).

Pleuro-coxal musculature

Ipcm4—M. propleuro-coxalis

O: Anterodorsal area of propleura, median of Idvm5 and Idvm6.

I: Anterio-medial procoxal rim.

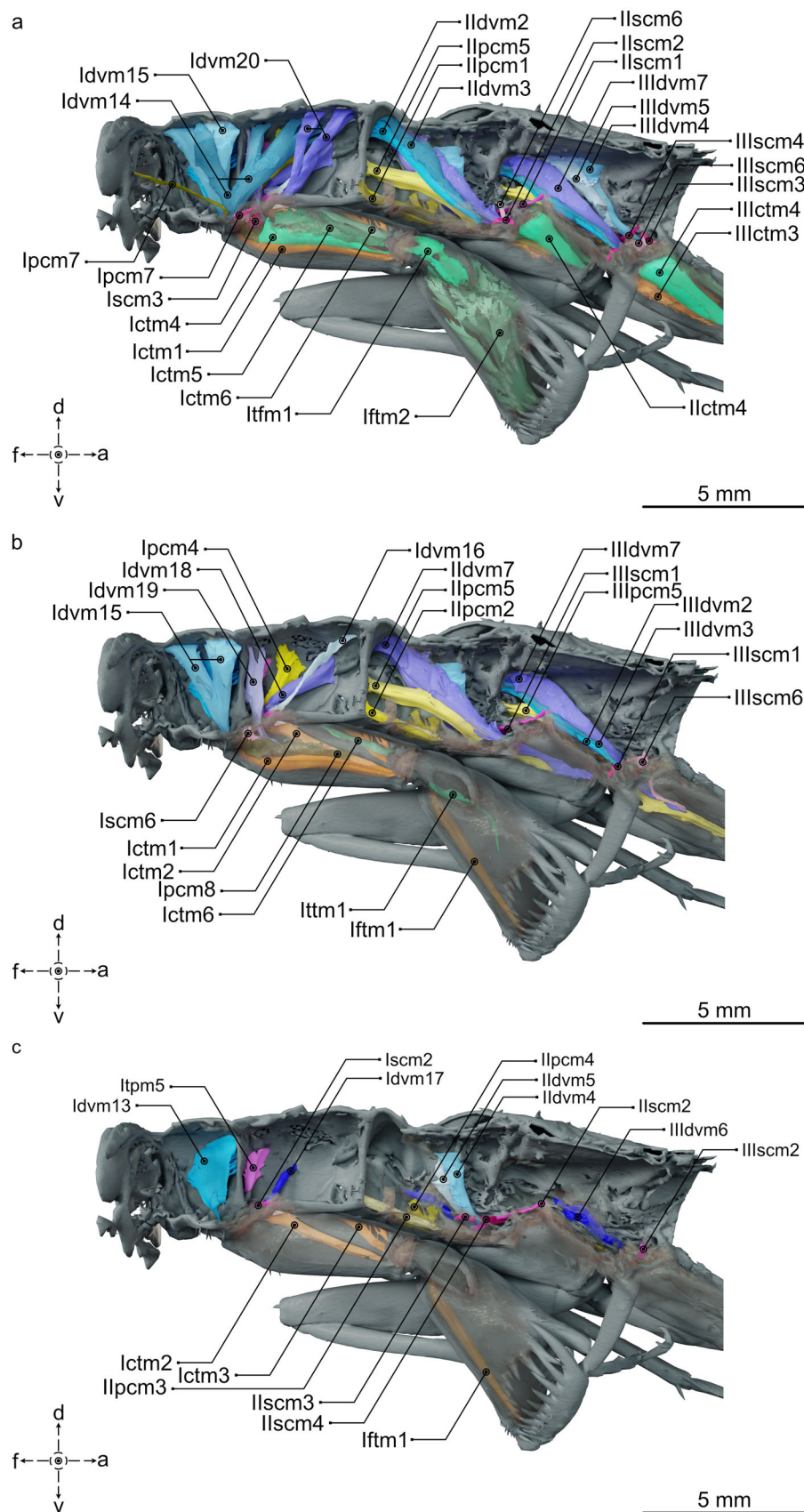


FIGURE 5 | Legend on next page.

Ipcm5—M. propleuro-coxalis inferior

O: Ventral face of propleural apodeme anterior to Ipcm6.

I: Antero-lateral procoxal rim.

C: Not present in Mantodea, but in *P. americana*.

Ipcm6—M. propleuro-coxalis posterior

O: Dorsal area of propleural apodeme.

I: Latero-medial procoxal rim.

C: Due to the connection between the intersegmental ridge via the propleural apodeme and the profurca in Mantodea, the muscle is very tiny; especially, in contrast to blattodeans, where the muscle is considerably larger.

Ipcm7—M. mesanepisterno-procoxalis transversalis

O: Median area of the intersegmental ridge between pro- and mesothorax.

I: Posterior procoxal rim of the opposite side.

C: In Mantodea, the muscle is only present in *Chaeteessa* sp. and *M. splendidus*. It is also present in *P. americana*.

Ipcm8—M. propleuro-trochanteralis

O: On the ventral area of the propleural apodeme.

I: Trochanteral extensor apodeme together with Idvm19, Iscm6, and Ictm5.

C: Together with the muscles Idvm19, Iscm6, and Ictm5 at the trochanteral extensor apodeme. The trochanteral extensor apodeme is much smaller and shorter in *P. americana*.

Sterno-coxal musculature

Iscm1—M. profurca-coxalis anterior

O: Most anterior part of the profurcal stem.

I: Antero-medial part of ventral procoxal rim.

Iscm2—M. profurca-coxalis posterior

O: Postero-lateral base of profurca.

I: Postero-median procoxal rim and same attachment point as Idvm16 and Ipcm6.

C: Not present in *P. americana*, but present in Mantodea.

Iscm3—M. profurca-coxalis medialis

O: Ventral face of profurca.

I: Medial procoxal rim.

C: Not present in *P. americana*, but present in Mantodea.

Iscm5—M. prospina-coxalis

O: Prospina.

I: Posterior procoxal rim.

C: Not present in Mantodea, but present in *P. americana*.

Iscm6—M. profurca-trochanteralis

O: Ventral face of profurca.

I: Together with the Idvm19, Ipcm8, and Ictm5 at trochanteral extensor apodeme.

C: Not present in *P. americana*.

Iscm7—M. prospinamesocoxalis

O: Prospina.

I: Anterior mesocoxal rim.

C: Not present in Mantodea, but present in *P. americana*.

Tergo-pleural musculature

Itpm4—M. pronoto-apodemalis anterior

O: Lateral region of the metazone of the pronotum, just posterior to the transversal ridge.

FIGURE 5 | Three-dimensional visualization of the extrinsic musculature in the thorax and the intrinsic musculature in the legs of an adult female *M. splendidus* from μ CT data in medial view. Partially, the cuticle is displayed transparent, to allow for a better view of the musculature in the back layers. Muscles are subsequently removed in every layer, to enhance an understanding of the spatial arrangement. Muscle M. profemoro-praetarsalis (Ifpm1) and the tibial muscles are not unambiguously markable in the μ CT data and therefore not displayed. (a) first layer; (b) second layer; (c) third layer. Additional interactive 3D models are available here: Extrinsic musculature of the prothorax (1 [<https://skfb.ly/p8FCJ>] and 2 [<https://skfb.ly/p8FCK>]), the mesothorax (1 [<https://skfb.ly/p8FCF>] and 2 [<https://skfb.ly/p8FCE>]), the metathorax (1 [<https://skfb.ly/p8FCD>] and 2 [<https://skfb.ly/p8FCG>]) and the intrinsic musculature of the forelegs (<https://skfb.ly/p8FCI>), midlegs (<https://skfb.ly/p8FCH>) and hindlegs (<https://skfb.ly/p8FCB>). a, abdominal; ctm, coxo-trochanteral muscle; d, dorsal; dvm, dorso-ventral muscle; f, frontal; ftm, femoro-tibial muscle; pcm, pleuro-coxal muscle; scm, sterno-coxal muscle; tfm, trochantero-femoral muscle; tpm, tergo-pleural muscle; ttm, trochantero-tibial muscle; v, ventral.

I: Dorsal face of procoxal rim.

C: Comparably short and far away from the coxa in *P. americana*, due to differing morphology of the furca and propleural apodeme in comparison to Mantodea.

Itpm5—M. pronoto-apodemalis posterior

O: Anterior region of prozone of the pronotum, postero-medial of the Itpm4.

I: Dorsal face of procoxal rim.

C: Comparably short and far away from the coxa in *P. americana*, due to differing morphology of the furca and propleural apodeme in comparison to Mantodea.

Intrinsic musculature of the (raptorial) forelegs (Figure 4 and 5).

Procoxa

Ictm1—M. procoxa-trochanteralis flexor anterior

O: Antero-dorsal procoxal surface.

I: Antero-dorsal base of the trochanter, together with Ictm2.

C: Comparably long in most mantodeans, in contrast to *Chaeteessa* sp., *M. splendidus* and *P. americana*.

Ictm2—M. procoxa-trochanteralis flexor medialis

O: Latero-dorsal procoxal surface.

I: Antero-dorsal base of the trochanter, together with Ictm1.

C: Within Mantodea only present in *Chaeteessa* sp. and *M. splendidus*. In *Chaeteessa* sp., it is comparably enlarged. Present in *P. americana*.

Ictm3—M. procoxa-trochanteralis flexor posterior

O: Posterior procoxal surface.

I: Postero-dorsal base of the trochanter.

C: In comparison to *P. americana*, much shorter in *M. splendidus* and insertion far more distal. Size and point of insertion in *Chaeteessa* sp. are somewhere between *P. americana* and *M. splendidus*. In the other mantodeans even shorter, insertion is very close to the coxa-trochanter joint.

Ictm4—M. procoxa-trochanteralis extensor anterior

O: Antero-ventral procoxal surface.

I: Antero-ventral base of the trochanter.

C: Within Mantodea, only present in *Chaeteessa* sp. and *M. splendidus*. Shorter and thicker in *M. splendidus* and *P.*

americana, due to the shape of the coxa. More slender in *Chaeteessa* sp.

Ictm5—M. procoxa-trochanteralis extensor medialis

O: Anterior procoxal surface.

I: At the trochanter extensor apodeme, together with Idvm19, Ipcm8, and Iscm6.

C: Dorsal to Ictm4, and shorter and thicker in *M. splendidus* and *P. americana*, due to the shape of the coxa. In *Chaeteessa* sp., it is as long as in other mantodeans, but comparably thicker.

Ictm6—M. procoxa-trochanteralis extensor posterior

O: Postero-ventral distal procoxal surface, close to the coxa-trochanter joint.

I: Postero-ventral base of the trochanter.

C: In comparison to the other mantodeans, very long in *M. splendidus* and *P. americana* with an attachment area much more distal. In *Chaeteessa* sp., it is even longer than in *M. splendidus* and appears more similar to *P. americana*.

Protrochanter

Itfm1—M. protrochanter-femoralis

O: Two-stranded and fan-shaped muscle, with a broad attachment area at the postero-ventral wall of the trochanter.

I: Proximal rim of the femur.

Ittm1—M. protrochanter-tibialis

O: Small muscle, with attachment at the anteroventral surface of the wall of the trochanter.

I: At the tibial flexor apodeme together with Iftm2 and 3.

Profemur

Iftm1—M. profemoro-tibialis dorsalis

O: Dorso-posterior area of the proximal femur.

I: Tibial extensor apodeme.

Iftm2—M. profemoro-tibialis ventralis ventralis

O: Anterior, along the ventral up until the posterior area of the proximal part of the femur.

I: Tibial flexor apodeme.

Ifpm1—M. profemoro-pretarsalis

O: Postero-lateral at the proximal end of femur.

I: Proximal end of tibial flexor apodeme.

C: Missing in *P. americana*, but present in Mantodea.

Tibia

Itipm1—M. protibio-pretarsalis

O: Distal third of the anterior tibial region.

I: Unguitractor plate (Aibekova et al. 2022; Gray and Mill 1985).

C: Not determinable in *Chaeteessa* sp. due to sample quality.

Itbm1—M. protibio-basitarsalis ventralis

O: Proximal, ventral area of the tibia.

I: Tibial articular process, next to Itbm2 (Aibekova et al. 2022).

C: Not determinable in *Chaeteessa* sp. due to sample quality.

Itbm2—M. protibio-basitarsalis anterior

O: Lateral tibial wall.

I: Tibial articular process, next to Itbm2 (Aibekova et al. 2022).

C: Not determinable in *Chaeteessa* sp. due to sample quality.

Itbm3—M. protibio-basitarsalis posterior

O: Ventral, distal region of the tibia.

I: Ventral, basal tarsal rim (Aibekova et al. 2022).

C: Not determinable in *Chaeteessa* sp. due to sample quality.

3.2 | Mesothorax

Extrinsic musculature of the mesothoracic legs (Figure 3, 5, and 7).

Dorso-ventral musculature

IIdvm2—M. mesonoto-trochantinalis anterior

O: Anterior part of mesonotum.

I: Trochantin, near trochantino-coxal joint.

C: Close to and difficult to distinguish from IIdvm3. Corresponds to Idvm13 in attachment area and functionality (see [Friedrich and Beutel 2008]).

IIdvm3—M. mesonoto-trochantinalis

O: Anterior part of mesonotum, posterior to IIdvm2.

I: Trochantin, near trochantino-coxal joint and posterior to IIdvm2.

C: Close to and difficult to distinguish from IIdvm2. Corresponds to Idvm14 in attachment area and functionality, but is not stranded (see [Friedrich and Beutel 2008]).

IIdvm4—M. mesonoto-coxalis anterior

O: Mesonotum and posterior to IIdvm2 and IIdvm3.

I: Posterior mesocoxal rim.

C: Close to IIdvm5, corresponds to Idvm16 in attachment area and functionality (see [Friedrich and Beutel 2008]). Thicker in *P. americana*.

IIdvm5—M. mesonoto-coxalis posterior

O: Posterior part of mesanepisternum, postero-lateral of IIdvm4.

I: Posterior mesocoxal rim, lateral of IIdvm4.

C: Close to IIdvm4, corresponds to Idvm17 in attachment area and functionality (see [Friedrich and Beutel 2008]).

IIdvm6—M. mesocoxa-subalaris

O: Posterior rim of mesocoxa

I: Subalare.

IIdvm7—M. mesonoto-trochanteralis

O: Central part of mesonotum, antero-lateral to IIdvm4.

I: Trochanteral tendon, together with Iipcm5, Iiscm6, and Iictm5.

C: Corresponds to Idvm19 in attachment area and functionality but is not stranded (see [Friedrich and Beutel 2008]).

Pleuro-coxal musculature

Iipcm1—M. mesanepisterno-trochantinalis

O: Antero-dorsal edge of mesanepisternum.

I: Trochantin.

C: Not present in *P. americana*.

Iipcm2—M. Mesobasalar-trochantinalis

O: Antero-dorsal part of mesanepisternum, posterior to Iipcm1, medial to Iipcm3.

I: Anterior mesocoxal rim.

C: Ventral to Iipcm3 in *P. americana*.

Iipcm3—M. mesanepisterno-coxalis anterior

O: Anterior part of mesanepisternum, lateral to Iipcm2.

I: Antero-lateral mesocoxal rim, close to Iipcm4.

C: Dorsal to Iipcm2 in *P. americana*.

Iipcm4—M. mesanepisterno-coxalis posterior

O: Antero-ventral half of mesanepisternum, lateral to Iipcm3.

I: Antero-lateral coxal rim.

C: Fan-shaped origin in mantodeans.

Iipcm5—M. mesanepisterno-trochanteralis

O: Antero-dorsal part of mesanepisternum, posterior to Iipcm3.

I: Trochanter, together with Iidvm7, Iiscm6, and Iictm5.

Sterno-coxal musculature

Iiscm1—M. mesofurca-coxalis anterior

O: Laterally on the base of mesofurcal stem.

I: Anterior mesocoxal rim.

Iiscm2—M. mesofurca-coxalis posterior

O: Lateral face of mesofurca stem.

I: Lateral face of posterior mesocoxal rim.

Iiscm3—M. mesofurca-coxalis medialis

O: Ventral face of mesofurcal arm, lateral of Iiscm6.

I: Medial face of posterior mesocoxal rim.

C: Not present in *P. americana*. but present in mantodeans.

Iiscm4—M. mesofurca-coxalis lateralis

O: Tip of mesofurcal arm.

I: Lateral face of mesocoxal rim.

C: Not present in *P. americana*., but present in mantodeans.

Iiscm5—M. mesospina-coxalis

O: Mesospina.

I: Posterior mesocoxal rim.

C: Not present in Mantodea, but present in *P. americana*.

Iiscm6—M. mesofurca-trochanteralis

O: Ventral face of mesofurca.

I: Together with the Iidvm7, Iipcm5, and Iictm5 at trochanteral extensor apodeme.

Iiscm7—M. mesospina-metacoxalis

O: Mesospina.

I: Anterior metacoxal rim.

C: Not present in Mantodea, but present in *P. americana*.

Intrinsic musculature of the mesothoracic legs (Figure 4, 5, and 7).

Mesocoxa

Iictm1—M. mesocoxa-trochanteralis flexor medialis

O: Postero-dorsal mesocoxal surface.

I: Postero-dorsal base of the trochanter, together with Iictm2.

Iictm2—M. mesocoxa-trochanteralis flexor posterior

O: Posterior mesocoxal surface.

I: Postero-dorsal base of the trochanter, together with Iictm1.

C: Fan-shaped in mantodeans. Area of attachment more distal in *P. americana*.

Iictm3—M. mesocoxa-trochanteralis flexor anterior

O: Antero-dorsal mesocoxal surface.

I: Antero-dorsal base of the trochanter.

Iictm4—M. mesocoxa-trochanteralis extensor anterior

O: Anterior mesocoxal surface.

I: Antero-ventral base of the trochanter.

Iictm5—M. mesocoxa-trochanteralis extensor medialis

O: Ventral mesocoxal surface, posterior to Iictm4 and anterior to Iictm6.

I: At the trochanter extensor apodeme, together with Iidvm7, Iipcm5, and Iiscm6.

C: Anterior attachment area for the origin in *P. americana*, dorsal of Iictm4.

Iictm6—M. mesocoxa-trochanteralis extensor posterior

O: Postero-ventral mesocoxal surface.

I: Postero-ventral base of the trochanter.

Mesotrochanter

IIfm1—M. mesotrochanter-femoralis

O: Two-stranded and fan-shaped muscle, with a broad attachment area at the postero-ventral wall of the trochanter.

I: Proximal rim of the femur.

IItm1—M. mesotrochanter-tibialis

O: Small muscle, with attachment at the antero-ventral surface of the wall of the trochanter.

I: At the tibial flexor apodeme together with IIfm2 and IIfm3.

Mesofemur

IIfm1—M. mesofemoro-tibialis dorsalis

O: Dorso-posterior area of the proximal femur.

I: Tibial extensor apodeme.

IIfm2—M. mesofemoro-tibialis ventralis ventralis

O: Anterior via ventral until the posterior area of the proximal part of the femur.

I: Tibial flexor apodeme.

IIfpm1—M. mesofemoro-praetarsalis

O: Postero-lateral proximal end of the femur.

I: Proximal end of tibial flexor apodeme.

C: Not present in *P. americana*.

Tibia

IItipm1—M. mesotibio-praetarsalis

O: Distal third of the anterior tibial region.

I: Unguitractor plate (Aibekova et al. 2022; Gray and Mill 1985).

IItbm1—M. mesotibio-basitarsalis ventralis

O: Proximal, ventral area of the tibia.

I: Tibial articular process, next to Itbm2 (Aibekova et al. 2022).

IItbm2—M. mesotibio-basitarsalis anterior

O: Lateral tibial wall.

I: Tibial articular process, next to Itbm2 (Aibekova et al. 2022).

IItbm3—M. mesotibio-basitarsalis posterior

O: Ventral, distal region of the tibia.

I: Ventral, basal tarsal rim (Aibekova et al. 2022).

3.3 | Metathorax

Extrinsic musculature of the metathoracic legs (Figure 3, 5, and 6).

Dorso-ventral musculature

IIIdvm2—M. metanoto-trochantinalis anterior

O: Anterior part of metanotum.

I: Trochantin.

C: Close to and difficult to distinguish from IIIdvm3. Corresponds to Idvm13 in attachment area and functionality (see Friedrich and Beutel [2008]).

IIIdvm3—M. metanoto-trochantinalis

O: Anterior part of metanotum, posterior to IIIdvm2.

I: Trochantin, close, and posterior to IIIdvm2.

C: Close to and difficult to distinguish from IIIdvm2. Corresponds to Idvm14 in attachment area and functionality, but is not stranded (see Friedrich and Beutel [2008]).

IIIdvm4—M. metanoto-coxalis anterior

O: Metanotum and posterior to IIIdvm2 and IIIdvm3.

I: Posterior metacoxal rim.

C: Close to IIIdvm5, corresponds to Idvm16 in attachment area and functionality (see Friedrich and Beutel [2008]).

IIIdvm5—M. metanoto-coxalis posterior

O: Posterior region of mesanepisternum, postero-lateral of IIIdvm4.

I: Posterior mesocoxal rim, lateral of IIIdvm4.

C: Close to IIIdvm4, corresponds to Idvm17 in attachment area and functionality (see Friedrich and Beutel [2008]).

IIIdvm6—M. metacoxa-subalaris

O: Posterior rim of metacoxa

I: Subalare.

IIIdvm7—M. metanoto-trochanteralis

O: Central part of metanotum, antero-lateral to IIIdvm4.

I: Trochanteral tendon, together with IIIpcm5, IIIscm6, and IIIctm5.

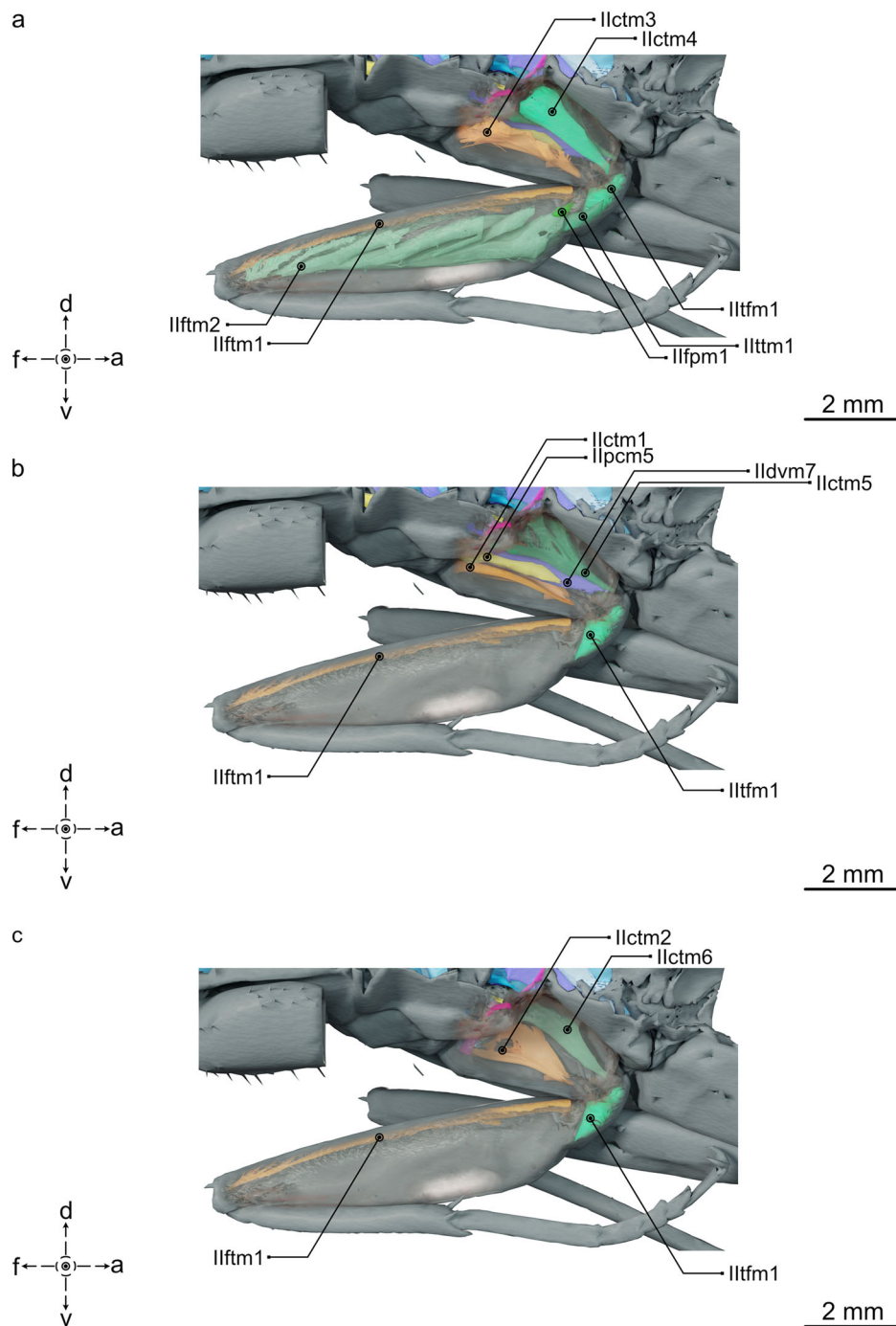


FIGURE 7 | Three-dimensional visualization of the extrinsic musculature in the mesothorax and the intrinsic musculature in the midlegs of an adult female *Metallyticus splendidus* from μ CT data in medial view. Partially, the cuticle is displayed transparent, to allow for a better view of the musculature in the back layers. Muscles are subsequently removed in every layer, to enhance an understanding of the spatial arrangement. The tibial muscles are not unambiguously markable in the μ CT data and therefore not displayed. (a) first layer; (b) second layer; (c) third layer. Additional interactive 3D models are available here: Extrinsic musculature of the mesothorax (1 [<https://skfb.ly/p8FCF>] and 2 [<https://skfb.ly/p8FCE>]) and intrinsic musculature of the midleg [<https://skfb.ly/p8FCH>]). a, abdominal; ctm, coxo-trochanteral muscle; d, dorsal; dvm, dorso-ventral muscle; fpm, femoro-praetarsal muscle; f, frontal; ftm, femoro-tibial muscle; pcm, pleuro-coxal muscle; tfm, trochantero-femoral muscle; ttm, trochantero-tibial muscle; v, ventral.

O: Antero-dorsal part of metanepisternum, posterior to IIIpcm1 medial to IIIpcm3.

I: Anterior metacoxal rim.

C: Ventral to IIIpcm3 in *P. americana*.

IIIpcm3—M. metanepisterno-coxalis anterior

O: Anterior part of metanepisternum, lateral to IIIpcm2.

I: Antero-lateral metacoxal rim, close to IIIpcm4.

C: Dorsal to IIIpcm2 in *P. americana*.

IIIpcm4—M. metanepisterno-coxalis posterior

O: Antero-ventral half of metanepisternum, lateral to IIIpcm3.

I: Antero-lateral metacoxal rim.

C: Fan-shaped origin in mantodeans.

IIIpcm5—M. metanepisterno-trochanteralis

O: Antero-dorsal part of metanepisternum, posterior to IIIpcm3.

I: Trochanter, together with IIIdvm7, IIIscm6, and IIIctm5.

Sterno-coxal musculature

IIIscm1—M. metafurca-coxalis anterior

O: Laterally on base of metafurcal stem.

I: Anterior metacoxal rim.

IIIscm2—M. metafurca-coxalis posterior

O: Lateral face of metafurcal stem.

I: Lateral face of the posterior metacoxal rim.

IIIscm3—M. metafurca-coxalis medialis

O: Ventral face of metafurcal arm, lateral of IIIscm6.

I: Medial face of posterior metacoxal rim.

C: Not present in *P. americana*, but present in mantodeans.

IIIscm4—M. metafurca-coxalis lateralis

O: Tip of metafurcal arm.

I: Lateral face of metacoxal rim.

C: Not present in *P. americana*, but present in mantodeans.

IIscm5—M. metaspina-coxalis

O: Metaspina.

I: Posterior metacoxal rim.

C: Not present in Mantodea, but present in *P. americana*.

IIIscm6—M. mesofurca-trochanteralis

O: Ventral face of metafurca.

I: Together with the IIIdvm7, IIIpcm5, and IIIctm5 at trochanteral extensor apodeme.

Intrinsic musculature of the metathoracic legs (Figure 4, 5, and 6).

Metacoxa

IIIctm1—M. metacoxa-trochanteralis flexor medialis

O: Postero-dorsal metacoxal surface.

I: Postero-dorsal base of the trochanter, together with IIIctm2.

IIIctm2—M. metacoxa-trochanteralis flexor posterior

O: Posterior metacoxal surface.

I: Postero-dorsal base of the trochanter, together with IIIctm1.

IIIctm3—M. metacoxa-trochanteralis flexor anterior

O: Antero-dorsal metacoxal surface.

I: Antero-dorsal base of the trochanter.

IIIctm4—M. metacoxa-trochanteralis extensor anterior

O: Anterior metacoxal surface.

I: Antero-ventral base of the trochanter.

IIIctm5—M. metacoxa-trochanteralis extensor medialis

O: Ventral metacoxal surface, lateral to IIIctm4.

I: At the trochanter extensor apodeme, together with IIIdvm7, IIIpcm5, and IIIscm6.

IIIctm6—M. metacoxa-trochanteralis extensor posterior

O: Postero-ventral metacoxal surface.

I: Postero-ventral base of the trochanter.

Metatrochanter

IIIftm1—M. metatrochanter-femoralis

O: Two-stranded and fan-shaped muscle, with a broad attachment area at the postero-ventral wall of the trochanter.

I: Proximal rim of the femur.

IIIttm1—M. metatrochanter-tibialis

O: Small muscle, with attachment at the antero-ventral surface of the wall of the trochanter.

I: At the tibial flexor apodeme together with IIIftm2 and IIIftm3.

Metafemur

IIIftm1—M. metafemoro-tibialis dorsalis

O: Dorso-posterior area of the proximal femur.

I: Tibial extensor apodeme.

IIIftm2—M. metafemoro-tibialis ventralis ventralis

O: Anterior via ventral until the posterior area of the proximal part of the femur.

I: Tibial flexor apodeme.

IIIIfpm1—M. metafemoro-pretarsalis

O: Postero-lateral proximal end of femur.

I: Proximal end of tibial flexor apodeme.

Tibia

IIIItipm1—M. metatibio-pretarsalis

O: Distal third of the anterior tibial region.

I: Unguitractor plate (Aibekova et al. 2022; Gray and Mill 1985).

IIIItbm1—M. metatibio-basitarsalis ventralis

O: Proximal, ventral area of the tibia.

I: Tibial articular process, next to Itbm2 (Aibekova et al. 2022).

IIIItbm2—M. metatibio-basitarsalis anterior

O: Lateral tibial wall.

I: Tibial articular process, next to Itbm2 (Aibekova et al. 2022).

IIIItbm3—M. metatibio-basitarsalis posterior

O: Ventral, distal region of the tibia.

I: Ventral, basal tarsal rim (Aibekova et al. 2022).

4 | Discussion

Our study documents the leg- and associated thorax morphology in Blattodea and Mantodea. We combined our original results with those of former studies (Alsop 1978; Bäumler, Gorb, and Büsse 2023; Carbonell 1947; Frantsevich 1998; Gray and Mill 1985; Levereault 1936; Maki 1938). These combined results demonstrate the importance of a comprehensive investigation of closely related taxa, to reveal general principles and facilitate the evolutionary understanding and relationship between anatomical structures. This becomes particularly clear when the data is considered in the context of highly derived and specialized modifications. In this comparative study, we initially updated the knowledge of the legs and associated thorax anatomy of *P. americana* (Blattodea) using its appendages

exclusively for locomotory function, as the primary function of legs in the majority of insects. Subsequently, we conducted a comparison to the blattodeans sister group, the praying mantises (Mantodea), whose members exhibit considerable transformations in the prothorax and forelegs, adapted for prey capture (cf. Bäumler, Gorb and Büsse [2023]).

Historically, the anatomy of blattodean legs (musculature set-up, cuticle structures, etc.) was studied by Maki (1938), Carbonell (1947) and Alsop (1978). However, previous research has yielded inconsistent results, complicating comparative approaches. Especially the elaborations of Carbonell (1947) proved to be extremely helpful and served as a primary reference for our comparisons. In Supporting Information S1: 1, we combined the information from previous works with our original results, transferring them into the current nomenclature system suggested by Friedrich and Beutel (2008) and Aibekova et al. (2022), thereby easing future comparative work that relies on musculature in Dictyoptera, and likely all Neoptera. By using the nomenclature of Friedrich and Beutel (2008), in agreement with Snodgrass (1935) definition of an individual muscle—considering a muscle as a functional group rather than individual fiber bundles—we propose a reduced set of extrinsic and intrinsic muscles in the thorax and all three pairs of walking legs for *P. americana* (Blattodea). In terms of extrinsic musculature, Friedrich and Beutel (2008) applied their nomenclature to the results from Carbonell (1947), which, in almost all cases, matches the data presented here. In that nomenclature system, *P. americana* shows an identical number of extrinsic and intrinsic muscles in the meso- and metathorax, though only concerning the sterno-coxal musculature, different muscles are present. It is important to mention that muscle Iscm7 serves a function in the mesothoracic leg, while IIs cm7 serves a function in the metathoracic leg. The same applies to muscle IIs cm5 (function in the metathoracic leg). The mesothoracic legs serve a critical role in maintaining stability and balance, especially while in a fast motion (mesothoracic legs spend the most time in contact with the ground), which is supported by the mentioned additional sterno-coxal muscle that connects the mesothoracic coxal rim to the spina between the pro- and mesothorax (Delcomyn 1971). In contrast, the metathoracic legs are the main propulsive units while running (Full & Tu 1990), which is supported by the sterno-coxal muscle IIs cm7, connecting the metathoracic coxal rim to the spina between the meso- and metathorax, as well as the two sterno-coxal muscles IIIs cm3 and IIIs cm4, connecting the furca to the lateral and medial metacoxal rim. The prothoracic legs serve a variety of different tasks, such as cleaning, sensing the environment in the direction of motion as well as enabling fast turning movements while in motion (Jindrich and Full 1999). This increased range of functions is made possible by a different set of extrinsic and a comparably increased number of intrinsic muscles, as well as a generally higher flexibility of coxal and sternal sclerites (Carbonell 1947; Hughes 1952). Additionally, the trochantine of the prothorax is comparably smaller and more flexibly connected to the adjacent episternum, resulting in increased flexibility of the procoxal joint. This flexibility is further enabled and supported by the increased number of dorso-ventral and pleuro-coxal muscles (e.g., the three-stranded muscle Idvm14 that inserts at the prothoracic trochantine). Concerning the intrinsic musculature, it is noteworthy that

except for one additional muscle in the procoxa (Ictm7), the number of muscles is identical in the three pairs of legs. Still, there is one peculiar difference between the first and the remaining pairs of legs. In the procoxa, muscle Ictm1—as one of the two anterior flexor muscles—is comparably thick and attached with the closely posterior situated slim and straight muscle Ictm2 at the anterior flexor apodeme. Muscle Ictm3, as the posterior flexor muscle, originates further distal on the posterior coxal wall and is attached to the posterior flexor apodeme. In contrast, in the pterothoracic legs, muscles II/IIIctm3 originate further distal than the other two flexor muscles (on the anterior coxal wall) and attach at the anterior flexor apodeme. The now posterior and broad flexor muscles II/IIIctm1 insert at the posterior flexor apodeme, together with the slim and straight muscles II/IIIctm2 situated posteriorly.

In the existing literature, 15 extrinsic and 15 intrinsic muscles were described in the mantodeans prothorax (Bäumler, Gorb, and Büsse 2023). We propose some changes to the presented musculature set-up, that became clear through the evolutionary analysis of *P. americana* (Supporting Information S1: 1). The sterno-coxal muscle, incorrectly described as Iscm2 (Bäumler, Gorb, and Büsse 2023), is indeed muscle Iscm4. Additionally, we confirmed the presence of muscle Iscm3, which corresponds to the sternal posterior coxal rotator in Gray and Mill (1985) and muscle 14 in Frantsevich (1998). Lastly, muscle Iscm6 as part of muscle 23 in Frantsevich (1998) and the pleural trochanteral extensor in Gray and Mill (1985), was missing in the previous analysis of Bäumler, Gorb and Büsse (2023) but proved to be present in all investigated species herein.

For the intrinsic muscles, we adapted the basic principles of the nomenclature system introduced by Friedrich and Beutel (2008) supplemented by the approach of Aibekova et al. (2022), applying it to the previous descriptions including our new results (Supporting Information S1: 1). After careful consideration of the insights gained from the comparison with *P. americana*, we decided to combine the femoral reductor a and b as well as the femoral tibial flexor pennate and parallel to one muscle (trochanter femur muscle 1 [tfm1] in the trochanter and the femur tibia muscle 2 [ftm2] in the femur) respectively (Bäumler, Gorb, and Büsse 2023; Gray and Mill 1985). This is supported by functional aspects, as the previously individual muscles are situated close to each other, have the same point of insertion and enable the motion of a monoaxial joint. Most changes to the previous descriptions were made to the musculature set-up in the coxa. From this, we were able to develop a classification, supported by the observed morphological features and comparison with the new data from *P. americana* (Figure 1c). We furthermore showed, that the muscle set-up is identical in the walking legs of *D. desiccata*, *M. religiosa* and *M. splendidus* and provided an overview of the present musculature (Supporting Information 1). The results obtained for the different Mantodea species were identical, except for the musculature of the prothorax and the raptorial forelegs in *Chaeteessa* sp. and *M. splendidus*. Although *M. splendidus* features the elongated prothorax and the associated spatial displacement of several muscles commonly found in Mantodea, it not only resembles cockroaches from its external appearance and muscle set-up but

additionally shows distinct differences from other investigated Mantodea species.

Interestingly, within Mantodea the cuticle structures of both meso- and metathorax, the associated legs, as well as extrinsic and intrinsic musculature, are identical throughout all investigated species. Except for the slightly enlarged coxa and trochanter, the cuticular structures and attachment points of the musculature appear to be fairly typical for insect walking legs and match previous descriptions (Friedrich and Beutel 2008). In the blattodeans, only slight differences are present: while the abductor muscles II/IIIscm3, as well as the remotor muscles II/IIIscm2, are missing in the pterothorax, and the promotor muscles II/IIIpcm1 are missing in the mesothorax of *P. americana*, the additional sterno-coxal muscles IIscm5 and I/IIscm7 were found. From their attachment points, it can be assumed that muscle IIscm5 fulfils a similar function to IIscm3 and Ipcm1, while muscles I/IIscm7 fulfill a similar function to II/IIIscm2. The differences may arise from the differing general posture of these insects' bodies—praying mantises tend to stand upright, while cockroaches keep their body pressed close to the ground—and tasks the pterothoracic legs are supposed to fulfill in both groups. While in the cockroaches, the mesothoracic legs are stabilizing the body in fast motions, they work together with the metathoracic legs in praying mantises during the prey-capturing process. In mantises, the pterothoracic legs are bound to support the whole body, as they only use the four pterothoracic legs for locomotion during prey capture. Noticeably, the only difference concerning intrinsic muscles is the missing of muscles II/IIIcsm1 in blattodeans, which are present in all mantodeans.

The prothorax and the associated raptorial forelegs of Mantodea in comparison, show strong modifications to a prey-capturing function. Noticeably, the pleural ridge is strongly enlarged, forming the transversal ridge to mechanically support the prothorax against the extreme forces produced by the muscles of the raptorial forelegs. The pleural ridge, the pleural apophysis emerging from it, along with the furca and the furcasternum, form a rather stiff ring across the prothorax, providing further mechanical support. Here, in comparison to the pterothorax, due to the elongation of the prothorax and the associated shifts of sclerites, the attachment areas of especially tergum-related muscles exhibit a vast displacement and several of the present muscles are strongly enlarged. The points of origin of extrinsic muscles of the prozone appear to shift anteriorly, while muscles attaching to the metazone exhibit a displacement in a posterior direction. Nevertheless, the relative spatial position of the musculature still allows for a confident alignment to the descriptions made by Friedrich and Beutel (2008). In contrast, the prothorax of the Blattodea appears to be similar to the pterothorax in terms of cuticular structures. The points of origin of the extrinsic muscles in *P. americana* match the descriptions provided by Friedrich and Beutel (2008). In mantodeans, especially the main promotor muscles Idvm13 and Idvm15 (not present in the mesothoracic legs of mantodeans), as well as the main remotor muscles Idvm16 and Idvm17, show a comparable increase in elongation and a vast enlargement of the point of origin (Bäumler, Gorb, and Büsse 2023; Gray and Mill 1985). Due to the increased size and weight of the raptorial forelegs in comparison to the rather thin walking legs, those enlargements

are presumably necessary to enable the fast and powerful movements of the raptorial forelegs. Praying mantises also show a huge range of procoxal motion in lateral and medial directions, which can be observed in their impressive defensive behavior, abducting the forelegs extremely far to display the anterior surface of coxa and femur as well as the ventral prothoracic sternites (Edmunds 1972; Yamawaki 2011). The high mobility is further necessary so that the mantis can clean the surface of the raptorial forelegs using its mouthparts (Zack 1978). In our analysis, an increased size (muscle Idvm18) and point of attachment of the abducting muscles were found in the prothorax (muscles Idvm18, Ipcm4, Ipcm6) (Bäumler, Gorb, and Büsse 2023; Gray and Mill 1985). Interestingly, the muscle Ipcm6 is missing in *M. splendidus*—although it is present in all other investigated Mantodea species—but similar to the *P. americana*, the muscle Ipcm7 is present (absent in other Mantodea). Likely, this is related to its cockroach-like lifestyle, hiding in crevices and running fast, similarly to a cockroach (Wieland 2008). Due to the flexible connection of both articulatory points, the coxal articulation gains a vast increase in movability, allowing for increased abduction-adduction, supination-pronation, as well as rotational movements (cf. Frantsevich [1998]). To enable this abducting motion, the lateral coxal joint is slightly rotated medial around the axis between the flexibly suspended connection of the pleural apophysis and the furca, thereby spatially shifted in a medial direction closing into the medial coxal articulation. As antagonists and to prevent an unwanted inwards displacement of the lateral coxal joint, muscles Itpm4 and Itpm5 attach to the lateral protrusion originating from the ventral part of the episternum. Here, due to the point of origin and point of insertion of muscles II/IIItpm4 and II/IIItpm5 in the pterothorax, both muscles are unlikely to contribute to the movements of the legs at all. Muscles Iscm1 and Idvm14 work as the antagonistic adductor muscles, with muscle Idvm14 being three-stranded in the prothorax, connected to the trochantine and therefore, the medial coxal articulation. Furthermore, more pleuro-coxal muscles are present in the pterothorax, with the muscles II/IIIpcm1, II/IIIpcm2, II/IIIpcm3 and II/IIIpcm4 contributing to promotion and abduction movements, while the muscles II/IIIpcm6 insert at the trochanteral rim and contribute to its extension. Concerning sterno-coxal muscles, one additional abductor (II/IIIscm4) is present in the pterothorax. In comparison, the blattodeans are missing the remotor muscles Idvm20 and Iscm2, the abductor muscle Iscm3, and the trochanteral extensor Iscm6. The present differing muscles Ipcm5, Ipcm7, and Iscm7 likely contribute all to an increased abduction mobility. As the prothoracic legs serve multiple different purposes in many insects (e.g., cleaning), next to locomotion, it is imaginable that they may profit from increased leg mobility.

The intrinsic muscles of *M. splendidus*, *Chaeteessa* sp. and *P. americana* show an intermediate state of muscle arrangements in the coxa in contrast to the other studied praying mantises (also Bäumler, Gorb and Büsse [2023]). The three first mentioned show a higher number of muscles, with three flexor muscles (muscles Ictm1, Ictm2, and Ictm3) and three extensor muscles (muscles Ictm4, Ictm5, Ictm6). In the later branching mantodeans, Ictm2 and Ictm4 are missing completely. In *P. americana*, muscle Ictm1 is a large muscle that is posteriorly accompanied by the slender muscle Ictm2, both inserting at the

anterior trochanteral flexor apodeme that fuses close to the trochanteral rim. While both of these muscles originate from the proximal inner wall of the coxa, the muscle Ictm3 originates further distal from the inner coxal wall, inserting at the posterior trochanteral rim. In *M. splendidus*, due to the elongated coxa, both muscles ctm1 and ctm2 are stretched while keeping the identical points of attachment in comparison to *P. americana*. In contrast, muscle Ictm3 appears to be smaller in comparison to *P. americana*, and its point of origin is shifted even further in the distal direction. In *Chaeteessa* sp., the origin of muscle Ictm3 is located somewhere in between—further distal than in *P. americana*, but noticeably further proximal in comparison to *M. splendidus*. In the other praying mantises investigated in this study and by Bäumler, Gorb and Büsse (2023), the alteration in these muscles is even more noticeable. In the other investigated mantodeans—excluding *Chaeteessa* sp. and *M. splendidus*—while muscle Ictm2 is missing entirely, due to the extreme elongation of the procoxa, the muscle Ictm1 is elongated, with its point of origin being distributed over a long area of the inner anterior coxal wall, inserting in the extremely elongated anterior trochanteral flexor apodeme. The muscle Ictm3 exhibits a similar trend: it is further shortened, with its point of origin being shifted close to the proximal end of the coxa. A comparable difference can be observed in the extensor muscles. In *Chaeteessa* sp. and *P. americana*, the anterior extensor muscle Ictm4 and the posterior extensor muscle Ictm6 are both broad muscles that originate from the proximal inner coxal wall, with muscle Ictm4 inserting at the anterior and Ictm6 at the posterior trochanteral rim. The extensor muscle Ictm5 originates on the anterior proximal inner coxal wall and inserts between the remaining extensor muscles at the trochanteral extensor apodeme, together with muscles Idvm19 and Ipcm8. An intermediate state can again be observed in *M. splendidus*, with an enlargement and stretching of the muscles Ictm4 and Ictm5, shortening of muscle Ictm6 and a shift of its point of origin towards the proximal end of the femur. Again, *Chaeteessa* sp. shows an intermediate state between *P. americana* and *M. splendidus*. Muscle Ictm5 is as long and stretched out as in the remaining mantodeans (excluding *M. splendidus*), but comparably thicker. Muscle Ictm6 is longer in *Chaeteessa* sp. than in *M. splendidus* and appears more similar to *P. americana*. Lastly, the alteration is even more pronounced in the remaining praying mantises, with muscle Ictm5 being extremely elongated and broadened, its point of origin covering a broad area of the ventral inner coxal wall and inserting in the considerably elongated trochanteral extensor apodeme. In comparison to the flexor muscles, the extensor muscle Ictm6 appears to be short with its point of origin being shifted close to the distal end of the coxa. During predatory strike, it is crucial to achieve a fast extension of the coxa-trochanter joint, to get the femur and tibia close to the prey and secure the catch (Copeland and Carlson 1979; Oufiero 2022; Oufiero et al. 2016; Prete, Klimek, and Grossman 1990). In the praying mantis' morphology, this is reflected in the number of muscles contributing to the extension, as well as in their size, which seems to be much larger in the raptorial forelegs in comparison to the pterothoracic walking legs.

In summary, in *P. americana*, the individual flexor and extensor muscles within the coxa (coxo-trochanteral muscles) of all three pairs of legs are of similar size and presumably

contribute equally to the movement of the associated trochanter during walking (extension and flexion). A similar state can be observed in the mantodean mid- and hindlegs, which is plausible as they are also used as locomotory appendages. In contrast, the majority of Mantodea (later branching species) show a reduction or shortening of certain muscles, and an enlargement of certain other muscles in the different parts of the forelegs—especially in the coxa—that are presumably related to the movement sequence during the predatory strike. Here, both flexor and extensor muscles are reduced to two respectively, where one of them is vastly enlarged (muscle Ictm1 and muscle Ictm5), while the other one is extremely shortened (muscle Ictm3 and Ictm6). The fast extension of the legs as well as the fast and powerful closure of the tibia on the femur seem to be important in the process, as the associated muscles are even more noticeably enlarged (especially Idvm19, Ipcm8, and Ictm5 as well as Iftm2) than the corresponding flexor muscles. The raptorial forelegs of the later branching mantodeans are mostly positioned in front of and dorsal of the mantises' body. During the movement, the intrinsic muscles ensure a fast and powerful movement in a straight line in front of the animal. This could be the reason for an enlargement of a few muscles, while other adjacent muscles are reduced. With the coxa being the first link in the kinematic chain, the extrinsic muscles of the prothorax are mainly responsible for adjustments during the strike and further provide increased flexibility during walking. Especially considering coxo-trochanteral muscles, an intermediate state of the described changes between the walking legs of *P. americana* and the later branching mantodeans was observed in *Chae-teessa* sp. and *M. splendidus*. This gradual change of morphological characteristics—from the walking legs in blattodeans up to the highly specialized prey capturing devices in later branching mantodeans—presumably represents the stepwise modification towards an additional new function (prey capturing) of the forelegs.

5 | Conclusions

In the pterothoracic exclusive walking legs of Blattodea and Mantodea, only minor differences could be found. In contrast, the comparison of the anatomy of the forelegs in both groups—walking forelegs in Blattodea and raptorial forelegs in Mantodea—has shown considerable differences. From a functional perspective, the main difference in the forelegs lies in the sclerites of the coxal articulation. In mantodeans, the mechanically reinforcing cuticular structures enable the implementation of powerful muscles while keeping a high movability of the coxal joint. This enables the praying mantises to take up an upright posture, carrying the forelegs ventrally of the body, facilitating a forward-facing predatory strike. Additionally, the enlarged musculature, with its broad points of origin, as well as their shifted attachment points, further contribute to differing requirements of motion in the raptorial forelegs. However, even with all these changes in the thorax anatomy, the allocation of tasks in single muscles for certain movements rather than several individual ones (e.g., in the intrinsic musculature of the coxa) and the high variability of the forelegs within Mantodea, praying mantises are

still perfectly capable of using all six legs for walking. Our examination of the selected taxa underscores the significance of broad investigations in elucidating general principles and deepening our understanding of character evolution, particularly when examining specialized and highly derived modifications.

Author Contributions

Fabian Bäumler: conceptualization, data curation, formal analysis, funding acquisition, investigation, methodology, project administration, resources, validation, visualization, writing—original draft, writing—review and editing. **Stanislav N. Gorb:** conceptualization, data curation, funding acquisition, project administration, resources, supervision, writing—review and editing. **Sebastian Büsse:** conceptualization, data curation, funding acquisition, investigation, methodology, project administration, supervision, validation, writing—review and editing.

Acknowledgements

We are grateful for the support of the members of the Functional Morphology and Biomechanics Group at Kiel University, particularly Esther Appel, Helen Gorges, Lena Marie Hindenberg, Alexander Köhnse and Benedikt Josten; as well as the Cytology and Evolutionary Biology group at the University of Greifswald, particularly to Christine Kiesmüller. We are especially thankful to Thies H. Büscher for many elucidating discussions. Furthermore, we want to thank Dr. Jessica L. Ware, Henry Uphoff, Marius Pohl and Markus Dammer for the provided specimens. Additionally, we would like to thank Alice Hüttmann, Leonie Busecrus, Linah Baumer and Anna Maria Rotermund for student assistance. F.B. is directly supported by the Hans Böckler Foundation. The project is partially financed by the German Research Foundation (DFG) project BU3169/3-1 under project number: 531828325.

Ethics Statement

The authors have nothing to report.

Conflicts of Interest

The authors declare no conflicts of interest.

Peer Review

The peer review history for this article is available at <https://www.webofscience.com/api/gateway/wos/peer-review/10.1002/jmor.70013>.

Data Availability Statement

All data supporting our findings are presented in the paper and the Supporting Information, respectively. The μ CT raw data can be made available from the corresponding author upon reasonable request.

References

- Aibekova, L., B. E. Boudinot, R. Georg Beutel, et al. 2022. "The Skele-tomuscular System of the Mesosoma of *Formica rufa* Workers (Hymenoptera: Formicidae)." *Insect Systematics and Diversity* 6, no. 2: 1–26. <https://doi.org/10.1093/isd/ixac002>.
- Alsop, D. W. 1978. "Comparative Analysis of the Intrinsic Leg Musculature of the American Cockroach, *Periplaneta Americana* (L.)." *Journal of Morphology* 158, no. 2: 199–241. <https://doi.org/10.1002/jmor.1051580206>.
- Ariyanto, M., C. M. M. Refat, K. Hirao, and K. Morishima. 2023. "Movement Optimization for a Cyborg Cockroach in a Bounded Space Incorporating Machine Learning." *Cyborg and Bionic Systems* 4: 0012. <https://doi.org/10.34133/cbsystems.0012>.

- Bäumler, F., S. N. Gorb, and S. Büsse. 2023. "Extrinsic and Intrinsic Musculature of the Raptorial Forelegs in Mantodea (Insecta) in the Light of Functionality and Sexual Dimorphism." *Journal of Morphology* 284, no. 6: e21590. <https://doi.org/10.1002/jmor.21590>.
- Bäumler, F., A. Koehnsen, H. T. Tramsen, S. N. Gorb, and S. Büsse. 2020. "Illuminating Nature's Beauty: Modular, Scalable and Low-Cost Led Dome Illumination System Using 3D-printing Technology." *Scientific Reports* 10: 12172. <https://doi.org/10.1038/s41598-020-69075-y>.
- Beutel, R. G., F. Friedrich, S.-Q. Ge, and X.-K. Yang. 2014. *Insect Morphology and Phylogeny: A Textbook for Students of Entomology*. Berlin, Germany; Boston, USA: Walter de Gruyter GmbH.
- Brannoch, S. K., F. Wieland, J. Rivera, K.-D. Klass, O. Béthoux, and G. J. Svenson. 2017. "Manual of Praying Mantis Morphology, Nomenclature, and Practices (Insecta, Mantodea)." *ZooKeys* 696, no. 3: 1–100. <https://doi.org/10.3897/zookeys.696.12542>.
- Burrows, M., S. R. Shaw, and G. P. Sutton. 2008. "Resilin and Chitinous Cuticle Form a Composite Structure for Energy Storage in Jumping By Frog-hopper Insects." *BMC Biology* 6, no. 1: 41. <https://doi.org/10.1186/1741-7007-6-41>.
- Büsse, S., T. H. Büscher, E. T. Kelly, L. Heepe, J. S. Edgerly, and S. N. Gorb. 2019. "Pressure-Induced Silk Spinning Mechanism in Web-spinners (Insecta: Embioptera)." *Soft Matter* 15, no. 47: 9742–9750. <https://doi.org/10.1039/C9SM01782H>.
- Carbonell, C. S. 1947. "The Thoracic Muscles of the Cockroach *Periplaneta Americana* (L.)." *Smithsonian Miscellaneous Collections* 107, no. 2: 1–23. <https://doi.org/10.1093/aesa/40.3.396>.
- Catania, K. C. 2018. "How Not to Be Turned into a Zombie." *Brain, Behavior and Evolution* 92: 32–46. <https://doi.org/10.1159/000490341>.
- Chapman, R. F. 1998. *The Insects: Structure and Function* (4th Edition). New York City, USA: Cambridge University Press.
- Copeland, J., and A. D. Carlson. 1979. "Prey Capture in Mantids: A Non-Stereotyped Component of Lunge." *Journal of Insect Physiology* 25, no. 3: 263–269. [https://doi.org/10.1016/0022-1910\(79\)90053-2](https://doi.org/10.1016/0022-1910(79)90053-2).
- Cranston, P. S., and P. J. Gullan. 2014. *The Insects: An Outline of Entomology*. Hoboken, USA: John Wiley & Sons, Ltd.
- Cullen, M. J. 1969. "The Biology of Giant Water Bugs (Hemiptera: Belostomatidae) in Trinidad." *Proceedings of the Royal Entomological Society of London. Series A, General Entomology* 44, no. 7–9: 123–136. <https://doi.org/10.1111/j.1365-3032.1969.tb00836.x>.
- Delclòs, X., E. Peñalver, A. Arillo, et al. 2016. "New Mantises (Insecta: Mantodea) in Cretaceous Ambers From Lebanon, Spain, and Myanmar." *Cretaceous Research* 60: 91–108. <https://doi.org/10.1016/j.cretres.2015.11.001>.
- Delcomyn, F. 1971. "The Locomotion of the Cockroach *Periplaneta Americana*." *Journal of Experimental Biology* 54, no. 2: 443–452. <https://doi.org/10.1242/jeb.54.2.443>.
- Demers-Potvin, A. V., H. C. E. Larsson, M. Cournoyer, and O. Béthoux. 2021. "Wing Morphology of a New CRETACEOUS PRAYIN G Mantis Solves the Phylogenetic Jigsaw of Early-Diverging Extant Lineages." *Systematic Entomology* 46, no. 1: 205–223. <https://doi.org/10.1111/syen.12457>.
- Dittmann, I. L., M. K. Hörnig, J. T. Haug, and C. Haug. 2015. "*Raptoblatta waddingtonae* n. Gen. Et n. Sp.—An Early Cretaceous Roach-like Insect With a Mantodean-type Raptorial Foreleg." *Palaeodiversity* 8: 103–111.
- Edmunds, M. 1972. "Defensive Behaviour in Ghanaian Praying Mantids." *Zoological Journal of the Linnean Society* 51, no. 1: 1–32. <https://doi.org/10.1111/j.1096-3642.1972.tb00771.x>.
- Frantsevich, L. 1998. "The Coxal Articulation of the Insect Striking Leg: A Comparative Study." *Journal of Morphology* 236, no. 2: 127–138. [https://doi.org/10.1002/\(SICI\)1097-4687\(199805\)236:2<127::AID-JMOR4>3.0.CO;2-2](https://doi.org/10.1002/(SICI)1097-4687(199805)236:2<127::AID-JMOR4>3.0.CO;2-2).
- Friedrich, F., and R. G. Beutel. 2008. "The Thorax of *Zorotypus* (Hexapoda, Zoraptera) and a New Nomenclature for the Musculature of Neoptera." *Arthropod structure & development* 37, no. 1: 29–54. <https://doi.org/10.1016/j.asd.2007.04.003>.
- Full, R. J., and M. S. Tu. 1991. "Mechanics of a Rapid Running Insect: Two-, Four- and Six-Legged Locomotion." *Journal of Experimental Biology* 156, no. 1: 215–231. <https://doi.org/10.1242/jeb.156.1.215>.
- Gorb, S. N. 2004. "The Jumping Mechanism of Cicada *Cercopis Vulnerata* (Auchenorrhyncha, Cercopidae): Skeleton–Muscle Organisation, Frictional Surfaces, and Inverse-Kinematic Model of Leg Movements." *Arthropod Structure & Development* 33, no. 3: 201–220. <https://doi.org/10.1016/j.asd.2004.05.008>.
- Gray, P. T. A., and P. J. Mill. 1985. "The Musculature of the Prothoracic Legs and Its Innervation in *Hierodula Membranacea* (Mantidea)." *Philosophical Transactions of the Royal Society of London. B, Biological Sciences* 309, no. 1140: 479–503. <https://doi.org/10.1098/rstb.1985.0094>.
- Grimaldi, D. 2003. "A Revision of Cretaceous Mantises and Their Relationships, Including New Taxa (Insecta: Dictyoptera: Mantodea)." *American Museum Novitates* 3412: 1–47. [https://doi.org/10.1206/0003-0082\(2003\)412<0001:AROCMA>2.0.CO;2](https://doi.org/10.1206/0003-0082(2003)412<0001:AROCMA>2.0.CO;2).
- Hörnig, M., C. Haug, J. Schneider, and J. Haug. 2018. "Evolution of Reproductive Strategies in Dictyopteran Insects—Clues From Ovipositor Morphology of Extinct Roachoids." *Acta Palaeontologica Polonica* 63, no. 1: 1–24. <https://doi.org/10.4202/app.00324.2016>.
- Hörnig, M. K., J. T. Haug, and C. Haug. 2017. "An Exceptionally Preserved 110 Million Years Old Praying Mantis Provides New Insights into the Predatory Behaviour of Early Mantodeans." *PeerJ (Corta Madera, CA and London)* 5, no. 7: e3605. <https://doi.org/10.7717/peerj.3605>.
- Hughes, G. M. 1952. "The Co-Ordination of Insect Movements." *Journal of Experimental Biology* 29, no. 2: 267–285. <https://doi.org/10.1242/jeb.29.2.267>.
- Hurd, L. E. 1999. "Ecology of Praying Mantids." In *The Praying Mantids*, Edited by F. R. Prete, H. Wells, P. H. Wells, and L. E. Hurd, 43–60. Baltimore, USA: Johns Hopkins University Press.
- Izquierdo-López, A., C. Kiesmüller, C. Gröhn, J. T. Haug, C. Haug, and M. K. Hörnig. 2024. "Patterns of Morphological Evolution in the Raptorial Appendages of Praying Mantises." *Insect Science*: 1–19. <https://doi.org/10.1111/1744-7917.13423>.
- Jayaram, K., and R. J. Full. 2015. "Cockroaches Traverse Crevices, Crawl Rapidly in Confined Spaces, and Inspire a Soft, Legged Robot." *Proceedings of the National Academy of Sciences USA* 113, no. 8: E950–E957. <https://doi.org/10.1073/pnas.1514591113>.
- Jindrich, D. L., and R. J. Full. 1999. "Many-Legged Maneuverability: Dynamics of Turning in Hexapods." *Journal of Experimental Biology* 202, no. 12: 1603–1623. <https://doi.org/10.1242/jeb.202.12.1603>.
- Legendre, F., A. Nel, G. J. Svenson, T. Robillard, R. Pellens, and P. Grandcolas. 2015. "Phylogeny of Dictyoptera: Dating the Origin of Cockroaches, Praying Mantises and Termites With Molecular Data and Controlled Fossil Evidence." *PLoS One* 10, no. 7: e0130127. <https://doi.org/10.1371/journal.pone.0130127>.
- Leverault, P. 1936. "The Morphology of the Carolina Mantis." *The University of Kansas Science Bulletin* 24, no. 13: 205–259.
- Liang, J.-H., P. Vrsansky, and R. Dong. 2012. "Variability and Symmetry of a Jurassic Nocturnal Predatory Cockroach (Blattida: Raphidiomimidae)." *Revista Mexicana de Ciencias Geológicas* 29, no. 2: 411–421.
- Loxton, R. G., and I. Nicholls. 1979. "The Functional Morphology of the Praying Mantis Forelimb (Dictyoptera: Mantodea)." *Zoological Journal of the Linnean Society* 66, no. 2: 185–203. <https://doi.org/10.1111/j.1096-3642.1979.tb01908.x>.
- Maki, T. 1938. "Study of the Thoracic Musculature of Insects." *Memoirs of the Faculty of Science and Agriculture, Taihoku Imperial University* 24, no. 1: 1–360.

- Oufiero, C. E. 2020. "Evolutionary Diversification in the Raptorial Forelegs of Mantodea: Relations to Body Size and Depth Perception." *Journal of Morphology* 281, no. 4–5: 513–522. <https://doi.org/10.1002/jmor.21118>.
- Oufiero, C. E. 2022. "Ontogenetic Changes in Behavioral and Kinematic Components of Prey Capture Strikes in a Praying Mantis." *Evolutionary Ecology* 36, no. 4: 541–559. <https://doi.org/10.1007/s10682-021-10135-8>.
- Oufiero, C. E., T. Nguyen, A. Sragner, and A. Ellis. 2016. "Patterns of Variation in Feeding Strike Kinematics of Juvenile Ghost Praying Mantis (*Phyllocrania Paradoxa*): Are Components of the Strike Stereotypic?" *The Journal of Experimental Biology* 219, no. 17: 2733–2742. <https://doi.org/10.1242/jeb.139675>.
- Prete, F. R. 1999. "Prey Capture." In *The Praying Mantids*, Edited by F. R. Prete, H. Wells, P. H. Wells, and L. E. Hurd, 194–223. Baltimore, USA: Johns Hopkins University Press.
- Prete, F. R., C. A. Klimek, and S. P. Grossman. 1990. "The Predatory Strike of the Praying Mantis, *Tenodera Aridifolia Sinensis*." *Journal of Insect Physiology* 36, no. 8: 561–565. [https://doi.org/10.1016/0022-1910\(90\)90024-A](https://doi.org/10.1016/0022-1910(90)90024-A).
- Romeis, B. 1989. *Mikroskopische Technik*. Munich, Germany: Oldenbourg Verlag.
- Rossoni, S., and J. E. Niven. 2022. "Braking Slows Passive Flexion During Goal-Directed Movements of a Small Limb." *Current Biology* 32, no. 20: 4530–4537.e2. <https://doi.org/10.1016/j.cub.2022.08.052>.
- Roy, R. 1999. "Morphology and Taxonomy." In *The Praying Mantids*, Edited by F. R. Prete, H. Wells, P. H. Wells, and L. E. Hurd, 19–40. Baltimore, USA: Johns Hopkins University Press.
- Snodgrass, R. E. 1935. *Principles of Insect Morphology*. New York City, USA: McGraw-Hill Book Company, Inc.
- Svenson, G. J., and M. F. Whiting. 2009. "Reconstructing the Origins of Praying Mantises (Dictyoptera, Mantodea): The Roles of Gondwanan Vicariance and Morphological Convergence." *Cladistics* 25, no. 5: 468–514. <https://doi.org/10.1111/j.1096-0031.2009.00263.x>.
- Weihmann, T., L. Reinhardt, K. Weißing, T. Siebert, and B. Wipfler. 2015. "Fast and Powerful: Biomechanics and Bite Forces of the Mandibles in the American Cockroach *Periplaneta americana*." *PLoS One* 10, no. 11: e0141226. <https://doi.org/10.1371/journal.pone.0141226>.
- Wieland, F. 2008. "The Genus *Metallyticus* Reviewed (Insecta: Mantodea). *Species*." *Phylogeny and Evolution* 1, no. 3: 147–170.
- Wieland, F. 2013. "The Phylogenetic System of Mantodea (Insecta: Dictyoptera)." *Species, Phylogeny and Evolution* 3, no. 1: 1–306.
- Yamawaki, Y. 2011. "Defence Behaviours of the Praying Mantis *Tenodera Aridifolia* in Response to Looming Objects." *Journal of Insect Physiology* 57, no. 11: 1510–1517. <https://doi.org/10.1016/j.jinsphys.2011.08.003>.
- Zack, S. 1978. "Description of the Behavior of Praying Mantis With Particular Reference to Grooming." *Behavioural Processes* 3, no. 2: 97–105. [https://doi.org/10.1016/0376-6357\(78\)90037-2](https://doi.org/10.1016/0376-6357(78)90037-2).
- Zhang, Z., J. W. Schneider, and Y. Hong. 2013. "The Most Ancient Roach (Blattodea): A New Genus and Species From the Earliest Late Carboniferous (Namurian) of China, With a Discussion of the Phylogenophy of Early Blattids." *Journal of Systematic Palaeontology* 11, no. 1: 27–40. <https://doi.org/10.1080/14772019.2011.634443>.
- Zhang, Z., Y. Zhang, J. Zhang, and Y. Zhu. 2019. "Structure, Mechanics and Material Properties of Claw Cuticle From Mole Cricket *Gryllotalpa Orientalis*." *PLoS One* 14, no. 9: e0222116. <https://doi.org/10.1371/journal.pone.0222116>.

Supporting Information

Additional supporting information can be found online in the Supporting Information section.